IEEE Access
Multidisciplinary | Rapid Review | Open Access Journal

Received July 8, 2020, accepted August 10, 2020, date of publication August 24, 2020, date of current version September 9, 2020.

Digital Object Identifier 10.1109/ACCESS.2020.3019138

Fiber Bragg Gratings for Medical Applications and Future Challenges: A Review

DANIELA LO PRESTI[1], (Student Member, IEEE), CARLO MASSARONI[1], (Member, IEEE), CÁTIA SOFIA JORGE LEITÃO[2,3], MARIA DE FÁTIMA DOMINGUES[3], (Member, IEEE), MARZHAN SYPABEKOVA[4], DAVID BARRERA[5], IGNAZIO FLORIS[6], LUCA MASSARI[7,8], CALOGERO MARIA ODDO[7,8], (Senior Member, IEEE), SALVADOR SALES[6], (Senior Member, IEEE), IULIAN IOAN IORDACHITA[9], (Senior Member, IEEE), DANIELE TOSI[10], AND EMILIANO SCHENA[1], (Senior Member, IEEE)

[1]Departmental Faculty of Engineering, Unit of Measurements and Biomedical Instrumentation, Università Campus Bio-Medico di Roma, 00128 Rome, Italy
[2]i3N, Department of Physics, University of Aveiro, Campus Universitario de Santiago, 3810-193 Aveiro, Portugal
[3]Instituto de Telecomunicações-University of Aveiro, Campus Universitário de Santiago, 3810-193 Aveiro, Portugal
[4]School of Medicine, Nazarbayev University, 010000 Nur-Sultan, Kazakhstan
[5]Department of Electronics, University of Alcalá, 28805 Alcalá de Henares, Spain
[6]Photonics Research Labs (PRL), iTEAM, Universidad Politécnica de València, 46022 València, Spain
[7]The BioRobotics Institute, Scuola Superiore Sant'Anna (SSSA), 56127 Pisa, Italy
[8]Department of Excellence in Robotics & AI, Scuola Superiore Sant'Anna (SSSA), 56127 Pisa, Italy
[9]School of Engineering, Johns Hopkins University, Baltimore, MD 21218, USA
[10]School of Engineering, Nazarbayev University, Nur-Sultan 010000, Kazakhstan

Corresponding author: Emiliano Schena (e.schena@unicampus.it)

This work was supported in part by INAIL (the Italian National Institute for Insurance against Accident at Work), through the BRIC (Bando ricerche in collaborazione) 2018 SENSE-RISC (Sviluppo di abiti intelligENti Sensorizzati per prevenzione e mitigazione di Rischi per la SiCurezza dei lavoratori) Project under Grant ID10/2018, in part by the UCBM (Università Campus Bio-Medico di Roma) under the University Strategic HOPE (HOspital to the PatiEnt) Project, in part by the EU Framework Program H2020-FETPROACT-2018-01 NeuHeart Project under Grant GA 824071, by FCT/MEC (Fundação para a Ciência e Técnologia) under the Projects UIDB/50008/2020 - UIDP/50008/2020, and by REACT (Development of optical fiber solutions for Rehabilitation and e-Health applications) FCT-IT-LA scientific action.

ABSTRACT In the last decades, fiber Bragg gratings (FBGs) have become increasingly attractive to medical applications due to their unique properties such as small size, biocompatibility, immunity to electromagnetic interferences, high sensitivity and multiplexing capability. FBGs have been employed in the development of surgical tools, assistive devices, wearables, and biosensors, showing great potentialities for medical uses. This paper reviews the FBG-based measuring systems, their principle of work, and their applications in medicine and healthcare. Particular attention is given to sensing solutions for biomechanics, minimally invasive surgery, physiological monitoring, and medical biosensing. Strengths, weaknesses, open challenges, and future trends are also discussed to highlight how FBGs can meet the demands of next-generation medical devices and healthcare system.

INDEX TERMS Biomechanics, biosensing, fiber Bragg grating sensors, minimally invasive surgery, physiological monitoring.

I. INTRODUCTION

The increase in life expectancy is directly related to improvements in the quality of life, healthcare delivery systems, and patient management. The aging of the population has placed demands on changes in the healthcare system, even more centered on the patient's engagement for health prevention [1], [2]. Recent scientific breakthroughs and technological advancements are changing the way diseases are diagnosed and treated. All these transformations are involved in the so-called Healthcare 4.0 revolution [3]. Innovative assistive devices, novel healthcare systems, wearables, and biosensors represent the key enabling technologies of such health digitalization, which is leading to patient-tailored treatments and personalized therapies [1]. As an emerging technology, fiber Bragg gratings (FBGs) are becoming

The associate editor coordinating the review of this manuscript and approving it for publication was Gustavo Callico.

increasingly attractive for sensing applications showing several advantages over the competitors [4], [5]. Indeed, FBGs are small, light, chemically inert, non-toxic, immune to electromagnetic interferences, and easily multiplexable [4], [6]. It is difficult to find all these distinctive features combine in the electrical sensors. Besides, the FBGs intrinsic sensitivity to strain and temperature enables their use in the measurement of clinically relevant parameters and in several medical branches [6]. Although the advantages of FBGs are widely recognized, open challenges still exist for their application in clinical practice [7]. The increasing attention given to FBGs by publications on the use of this technology in the field of medicine and healthcare underlines the strong interest to fulfill the gap between research and clinical practice [7], [8].

This paper aims at giving an overview of the FBGs-based sensing solutions, their principle of work, and their most recent applications in medicine. A similar overview of the current state-of-the-art can offer a better understanding of the FBGs great potentialities while also underlining weaknesses and strengths of this technology. Moreover, issues and challenges which have dampened the FBGs clinical acceptance are discussed to promote the development of innovative FBGs-based sensing solutions for personalized healthcare and precision medicine.

The remainder of this review is divided as follows. Section II provides a description of the theoretical background and the measuring principles of the FBGs-based systems applied to medicine. Section III gives an overview of the state-of-the-art of the FBGs applications in biomechanics, minimally invasive surgery (MIS), physiological monitoring, and medical biosensing. Section IV includes a discussion of hurdles, open challenges, future trends, and final remarks to foster the use of FBGs in clinical settings.

II. THEORETICAL BACKGROUND AND MEASUREMENT PRINCIPLE

An FBG sensor is an optical resonator inscribed into the core of a fiber optic [9], [10]. The key principle of operation is to induce, by means of an external laser and an interferometer or a diffractive element, a periodic perturbation of the effective refractive index (n_{eff}) of a single-mode optical fiber, thereby causing a distributed interference between waves propagating forward and backward through the structure. Fig. 1a shows the main configurations of FBGs proposed for medical applications, their spectral response, and the parameters that they can directly measure [11], [12].

The simplest configuration is the uniform FBG [10], in which the modulation of n_{eff} has a constant period (Λ) along the fiber length z. This structure resonates at the so-called Bragg wavelength $\lambda_B = 2n_{eff}\Lambda$. The spectrum reflected by the FBG shows a steep peak centered around λ_B, with reflectivity usually within 10% and 90% in FBGs having a length ranging from 3 mm to 10 mm. For FBGs operating around 1550 nm, the reflected bandwidth is in the order of 0.3 nm; hence, an FBG sensor behaves similarly to a microwave notch filter having quality factor $\sim$ 5200 [9].

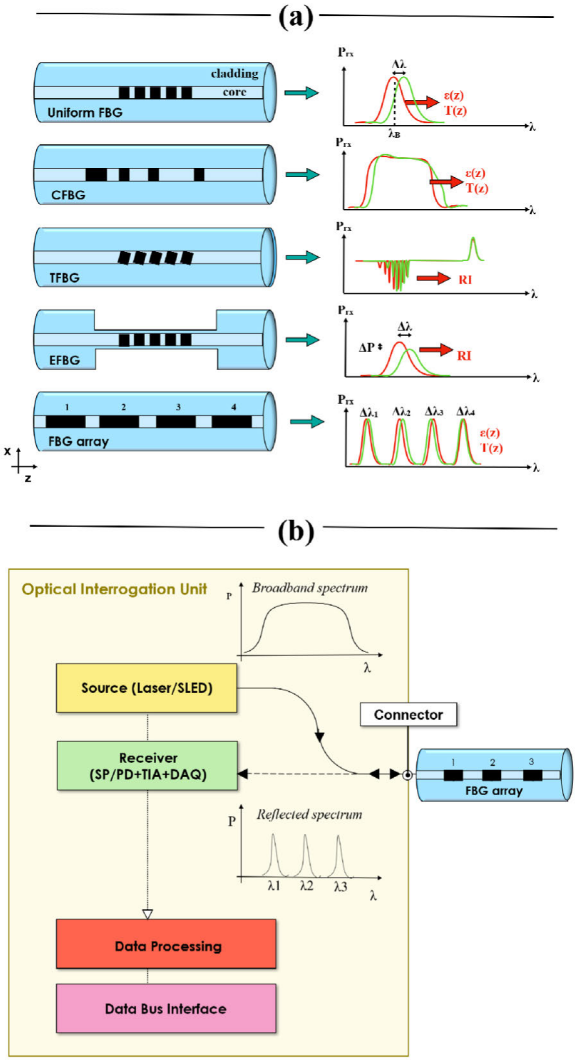

FIGURE 1. (a) The main configurations of FBGs: uniform FBG, CFBG, TFBG, EFBG, and FBG array. The spectral responses and measured parameters (strain - ε, temperature - T, refractive index - RI) are also reported. (b) A schematic representation of the interrogation unit with all the components used to interrogate and read the FBGs. An FBG array is shown by way of example. The data acquisition hardware -DAQ- in the receiver block is used to maintain the synchronization between the swept laser source and the array of photodetectors.

The measurement principle of the FBGs relies on the dependence of both n_{eff} and Λ on strain and temperature [9]–[12]: a grating tension or compression along its z-axis, as well as a temperature variation, cause a shift of the λ_B ($\Delta\lambda$), and of the whole spectrum.

The $\Delta\lambda$ has a linear dependence on both strain and temperature changes; for glass fibers operating in the infrared, typical sensitivity values are around 1 pm/$\mu\varepsilon$ for strain and 10 pm/°C for temperature changes. The optical fiber embedding the FBG needs a physical connection to a channel of a dedicated device (i.e., optical interrogator) by means of a standard connector (see Fig. 1b). The commercially available interrogators have a number of channels ranging from 1 to 16. Typically, FBGs are interrogated through a rapid scanning

tunable laser coupled to a photodetector (PD) followed by a transimpedance amplifier (TIA) or a broadband source like a superluminescent LED, (SLED) coupled to a spectrometer (SP) [12]. These systems allow the detection of the whole reflection spectrum, and using a peak-tracking method, it is possible to estimate the λ_B with an accuracy $\leq$ 1 pm. A schematic of the experimental setup used to interrogate FBGs is illustrated in Fig. 1b.

A chirped FBG (CFBG) is characterized by a non-uniform modulation $\Lambda = \Lambda(z)$; noteworthy in a linear CFBG the period of the grating increases at a constant rate through the grating length [13]. As a result, the CFBG does not reflect a single wavelength, but the spectrum has a broad bandwidth. Each portion of the grating reflects a different Bragg wavelength $\lambda_B(z) = \lambda_B(0) + \zeta z$, where ζ is the chirp rate [13], [14]. Since the CFBG behaves as a broadband reflector, in which each section has its own dependence on temperature or strain, CFBG sensors have been used to measure either temperature or strain distributions along the grating length z. The main approach, called spectral reconstruction, is based on an optimization technique [14]–[16]. This method estimates the temperature or strain distribution along the grating length (from 15 mm to 50 mm) by reading the spectral deformations from the reference conditions.

To make the grating sensitive to refractive index changes for biosensing applications, two main configurations have been exploited. The first approach is the use of a tilted FBG (TFBG), whereas the refractive index modulation plane is tilted with respect to the fiber axis by angles usually lower than 10° [17]–[19]. This grating has a λ_B similar to a standard FBG sensor, but also excites several cladding modes at the boundary between the cladding and the outer medium, that propagate out of the fiber. These modes are visible in reflection by coating the fiber with an end-reflector, such as a gold mirror, and appear as a comb of narrow linewidths at wavelengths smaller than λ_B [18]. The second approach is the etched FBG (EFBG), in which a uniform FBG is modified by chemically etching the fiber cladding along the grating [20], [21]. In EFBG, the poor light confinement causes a change of n_{eff} term as a function of the refractive index, depending on the fiber thickness. As a result, we observe both a $\Delta\lambda$ and a variation of the optical intensity, when the grating is exposed to refractive index changes [20].

The reflected bandwidth of FBGs is much smaller than the working range of the interrogators. Hence, it is possible to fabricate several grating elements along the fiber, in an array format, each having a different λ_B. In this principle, called wavelength division multiplexing (WDM), multiple FBGs are stacked in a single fiber. The use of this solution allows resolving the parameter of interest (e.g., temperature, strain, refractive index) along the fiber, isolating each FBG sensor contribution [22]. The FBG arrays can be fabricated with a custom density of sensors and achieve high resolution (e.g., sub-centimeter) for lengths up to several meters. Moreover, their behavior can be described by exploiting finite element models (FEMs) and combining experimental data with machine learning methods [23], [24].

All the aforementioned FBG configurations are designed as short-length distributed sensors which resonate at wavelengths that correspond to the propagation within the FBG pitch. Otherwise, the long period gratings (LPGs) have length longer than FBGs and resonate at $m\lambda_{LPG} = (n_{eff} - n^i_{cladding})\Lambda$ with m the order of coupling and $n^i_{cladding}$ the refractive index of the i mode of the cladding. Thus, LPG's behavior is more similar to multipath transmission interferometers (e.g., Mach-Zender) and LPGs have not been included in this work.

III. APPLICATIONS IN MEDICINE

A. BIOMECHANICS

The term biomechanics involves the application and the extension of mechanics to the human body at different levels of increasing complexity. In this section, an overview of FBGs-based systems for biomechanical applications will be given tracing the body structural organization, from the tissue level up to the system level [25]. The description will start with studies concerning soft and hard tissue responses to mechanical stimuli. Then, FBGs involved in musculoskeletal applications in terms of joint kinematics and pressure mapping will be reviewed. Lastly, works related to the interaction between native biological tissues and foreign materials (i.e., prostheses and orthoses) in terms of load transferring mechanisms and pressure distributions will be described. Fig. 2 shows the body parts involved in the following studies grouped into three main categories (i.e., Soft and Hard Tissue, Musculoskeletal System, and Prostheses, Orthoses, and Bone Cement). Each category is coded by a different color (i.e., green, bright blue, and pink, respectively).

1) SOFT AND HARD TISSUES

In the last decades, FBGs have been used to measure strain-stress fields in soft and hard tissue biomechanics, where conventional sensors are not technically feasible [5]. The principal aim is to extend the knowledge about the tissue mechanical properties useful to develop detailed analytic models and optimized sensing solutions. The term soft tissues mainly refer to ligaments, tendons, and muscles. In the literature, most of FBG-based applications in this field have concerned the measurement of strain and force of ligaments and tendons from both animals and cadavers [26], [27]. Gratings have been embedded into micro-fabricated encapsulations made of shape memory alloys [27], stainless steel [28], or directly attached to the tissue [28]. The systems' response to applied loads and controlled strains have been monitored during static and dynamic conditions to find out the systems' metrological characteristics. For instance, an FBG sensor housed into a micro-fabricated encapsulation made of shape memory alloy in [27] and of stainless steel in [28] was fabricated for strain and force sensing.

Tests in static and dynamic conditions (e.g., at different loads and during loading-unloading cycles to simulate

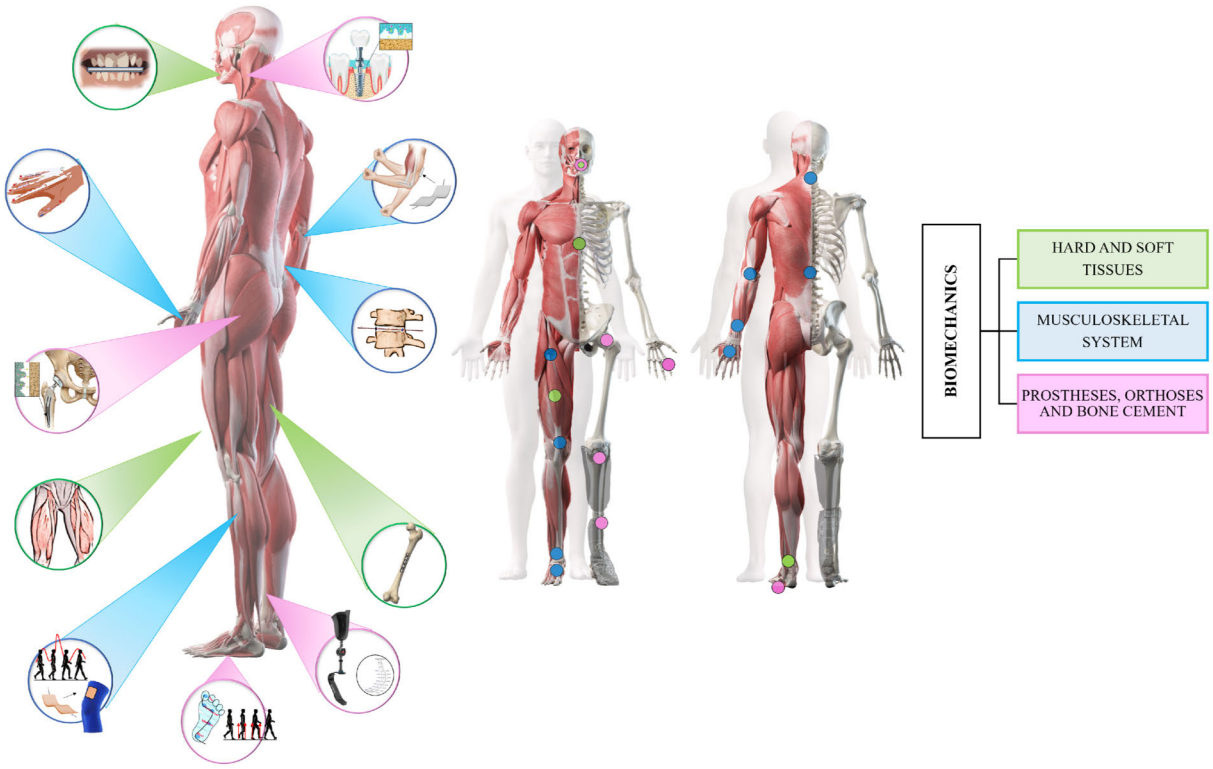

FIGURE 2. Applications in biomechanics. Examples of systems for soft and hard tissues are highlighted in green, for musculoskeletal system in bright blue, and for prostheses, orthoses, and bone cement in pink.

various postures and locomotion) were performed on a femoral cadaveric tendon and a ligament in [27], and on a bovine tendon in [28]. Results demonstrated good sensitivity, accuracy, and repeatability of the proposed systems that added to an easily implantability make these technological solutions adaptable for minimally invasive measurements. In other studies presented in [26] and [29], similar tests were performed to validate FEMs. In [26], a good correlation was found between the tendon strain distribution simulated by the proposed FEM and the one measured by an E-shaped buckle transducer (with an FBG sensor glued on its central arm). However, better results may be achieved using an array of multiplexed FBGs to allow distributed strain measurements. Not only the biomechanics of soft tissues from the lower limbs but also from other body districts have been studied in the literature. Recently, an FBG encapsulated in a protective sheath was used for measuring chordae tendineae tension in the cardiac mitral valve [30]. The sensor shape and movement mimicked the ones of the native biological tissue. Results of tests performed on both a 3D-printed left heart simulator and six independent chordae of a porcine mitral valve showed good performances and no interferences among chordae, during normal and hypertension-simulated conditions. Lastly, also *in-vivo* measurements of longitudinal and transverse strains and changes in the muscle-tendon unit were performed in [31]–[33]. In all these applications, FBGs were directly attached to the skin, and Magnetic Resonance (MR) images of the inner tissues were acquired.

Research efforts have also been dedicated to studying the biomechanics of hard tissues: bones and teeth. Bone deformations were investigated in response to applied loads [34]. Moreover, the influences of simulated fractures, bone decalcification, and sensor positioning layout on the strain measurements were studied [35], [36]. Synthetic and cadaveric femurs were employed, and strain gauges were often used as reference instruments. For instance, a total of four FBGs and four strain gauges were placed around the circumference of an acryl tube and a cadaveric femur bone of the same length. Results showed a loss of linearity by comparing results from sensors placed on the tube with the ones on the tissue. These findings reflect the genuine non-linearity in the bone segment. The measurement of strain as a quantitative evaluation of the effect of simulated fractures was presented in [35] and [36]. In [35], a total of seven FBGs were glued along a stainless-steel plate used to fix the fracture. FBGs resulted easier to use than strain gauges sensors, with higher feasibility to monitor the evolution of the strain in the bone. In [36], an array of FBGs was directly attached over fractured synthetic femur sawbones, and the influence of fiber orientation and gratings location on the strain measurements was investigated. Results suggested that a straight layout works better than a coiled one for strain sensing. Also, bone decalcification over time was analyzed as an influencing

factor in the strain measurement [37]. The comparison of FBG's output changes detected on an untreated sample and on a partially decalcified one showed a linear increase of strain with the calcium loss. In the literature, other applications of FBG-based systems in hard tissue biomechanics have concerned the measurement of deformations of teeth and mandible during mastication [38], [39]. In particular, the capability of monitoring clinically relevant bite forces in thirty-six volunteers, as well as detecting different masticatory patterns associated with the chewed food in animals was investigated. Results showed good performances for both the proposed systems. In [38], the bite force of males experienced higher values than females with the maximum force at the molar region; in [39], the output of an FBG sensor embedded in a titanium mesh showed a high signal-to-noise ratio useful to easily determine the magnitude and the frequency contents associated to the chewing process.

Precisely at the halfway between soft and hard tissues, it is located the articular cartilage. The mechanical properties of this tissue were studied in [40]–[42]. In all these works, the cartilage has been modeled using a viscoelastic model, and micro-indenters with an FBG sensor located at the tip were used to study changes in tissue relaxation times and stiffness. In [40] and [41], results showed an increase of all these parameters with the indentation depth. The spherical tip showed advantages in terms of shorted indenter length and risk minimization of tissue surface damage. The spherical indenter was also able to distinguish healthy cartilage from artificially degenerated in [42], and from osteoarthritic tissue of seven patients underwent knee replacement in [43]. Higher forces in [42], as well as higher stiffness in [43], were exhibited by the healthy cartilage. Otherwise, no significant differences were found in terms of relaxation times of tissues with different grades of degeneration [43].

2) MUSCULOSKELETAL SYSTEM

The inherent connectivity between soft and hard tissues is essential for musculoskeletal motion and stability. Indeed, at a higher level of complexity, the human body can be considered a whole-joint organism where bones meet and are functionally integrated with soft tissues to constitute a kinematic chain. In the literature, a lot of biomechanical studies focused on FBG-based systems for human joint kinematics. The principal clinical aims are the prompt detection of bad postural habits, which may lead to musculoskeletal diseases, and the quantitative assessment of the rehabilitation programs to provide even more personalized treatments.

Optical goniometers have been proposed for monitoring knee, elbow, and ankle range of motions (ROMs) [38], [44], [45], during static and dynamic conditions (e.g., static postures and walking). In all these works, cantilevers-based systems and different transmission mechanisms (e.g., stiff arms and rubber belts) were used for de-amplifying the strain transmitted to the grating, according to the ROM of the joint under investigation. The influence of the distance between a pin mechanism and a cantilever on the sensitivity of a custom optical goniometer was investigated in [43]. Results showed the bigger the distance, the higher the strain induced on the grating. Moreover, tests on twenty-six volunteers wearing the proposed device on the knee showed a good agreement between the output of the FBG-based goniometer and the one of the reference system in monitoring flexion/extension (F/E) movements. Moreover, a good accordance in the measurement of gait parameters during walking on either leg was achieved. Similar results were found in [38], where F/E movements of elbow and ankle were monitored by using an optical goniometer with rubber-based transmissions. However, all these solutions are bulky thus should be re-evaluated in terms of the user's comfort and ability to keep its rotation axis during gait trials.

For this reason, most of the studies for joint kinematics focused on the development and assessment of wearables based on FBGs [46]–[48] Usually, to improve their robustness and performances, FBGs have been housed into more flexible structures made of polymers such as Polyvinyl chloride - PVC [46]–[48], Dragon Skin^{TM}silicone families [49], [50], polylactic acid - PLA [51], and Thermoplastic Polyurethane (TPU) [52]. Buttons, belts, Velcro®strips, and tapes have been used as bonding elements.

ROMs and movement patterns have been monitored on both lower and upper limbs and spinal cord segments. Goniometers and motion capture systems have been often used as benchmarks. Several works focused on lower limbs to study their kinematics and understand the complex dynamics associated with the gait. Usually, the metrological characteristics of the wearable systems have been reported, followed by tests on a treadmill during walking, jogging and/or running. Among others, a wearable solution comprising a Kinesio Tape®(K-Tape) embedding an FBG sensor was proposed in [53] to monitor the angular displacement of the knee joint during gait cycles. Results showed the consistency of this solution to perform gait analysis and perceive the pick activity movements of the quadriceps. Some concerns of the proposed system are related to its fragility because the FBG was embedded bare. Thus, a step forward was done in [54], where an epoxy resin matrix was used to house the FBG, and two 3D-printed hooks were used to guarantee the sensor compliance with the K-Tape on the ankle. Another study proposed FBGs embedded in PVC strips to be worn on the elbow, knee, wrist, and back, in static angle posture maintenance and jogging tests [47]. Results showed stable output changes in response to step-by-step angular variations, and the elbow was the joint most affected by disturbances. During jogging, the sensor mounted on the knee showed the highest values of strain and a signal amplitude reduction with speed. In this context, an innovative fabrication technique was proposed to develop a smart ring for knee and elbow joints in [51]. The FBGs were encapsulated in the system made of PLA during the printing process. Then, different bend angles were performed to retrieve the FBG sensitivity and to assess the capability of monitoring movement patterns.

Wearables were also proposed for monitoring the mobility of phalanges of hands and feet. An instrumented rubber cable for monitoring plantar dorsiflex was fabricated in [55] whereas a smart glove in [56], and a smart TPU guide in [52] were used for interphalangeal joints movements detection. In [56], an array of fourteen FBGs embedded in PVC was glued in a coiled layout over the interphalangeal joints on the glove upper surface. Results reported minimum and maximum strains for fully opened and closed hands, respectively, with the need of a pre-calibration when worn by different subjects [56]. The capability of accurately distinguishing among metacarpophalangeal, distal and proximal interphalangeal (DIP and PIP) was confirmed in [56], but slight losses of linearly in the system response were found with finger size reduction. In [52], an array of thirty-six FBGs in a TPU guide was worn, assuring the contact with each finger by a tape on the nail on one side, a Teflon flattener on the opposite side, and a silicon ring structure around the guide. Results of the angular displacements response vs. torques (calculated by multiplying applied forces and moment arm) allowed the evaluation of the joint quasi-stiffness. Lastly, some studies investigated the use of FBG-based flexible sensors directly attached to the skin or taped on stretchable belts for spinal motion detection [50], [57]. In [50], the movements of F/E and axial rotation (AR) of the cervical segment of nine volunteers were detected by using two custom flexible sensors based on FBGs showing good performances when compared to a Motion Capture (MoCap) system used as a reference, with potentiality in preventing neck pain.

Another function of the musculoskeletal system regards body stability. In this arena, FBGs-based systems were used to monitor intravertebral discs (IVDs) pressure [58]–[61]. The IVDs are the main joints of the spinal segment, and an understanding of the pressure distribution is an essential indicator of disc mechanics, injuries, and degeneration etiology. In [59], the IVD nucleus pressure was measured by an optical probe with the grating at the tip. The optical system exhibited good repeatability in monitoring pressure and an easier insertion than strain gauges, which often causes interferences with the vertebral endplates and potential damages. Also, the influence of the insertion depth and the diameter of the probe on the measured pressure was described in [60], [61]. The probe was constituted by two segments joined together by means of a bar with an FBG glued above. At the same level of insertion, results showed that the bigger the diameter, the higher the forces, while at different levels, the deeper the insertion, the higher the force.

3) PROSTHESES, ORTHOSES, AND BONE CEMENT

Other applications of FBGs for human biomechanics are related to the study of the interaction between human inner/outer tissues and foreign materials. The main aims are the recovery optimization of lost musculoskeletal functions through the replacement of body parts (i.e., prostheses) and the improvement of residual functions through the application of external devices designed to fit with the outer body components (i.e., orthoses).

Pressure mapping and strain distribution at the prosthetic joints have been measured to study malalignments and/or unbalanced contact area [62]–[64]. For instance, two arrays of five CFBGs each were embedded in a tibial spacer to map the pressure on cadaveric condylar grooves during a total knee replacement. Results of non-uniform pressure mapping suggested a failure of knee arthroplasty with risky long-term degradation of the bones in *in-vivo* applications. Moreover, the fiber diameter, the presence of bone cement, and the use of press-fit prophylactic stems were investigated as influencing factors on load transferring and strain distributions at the implant-femur interfaces in [58], and [65], respectively. Results showed that a small fiber diameter improved the sensing element performance, a cemented prosthesis allowed a more uniform distribution of the pressure, and a press-fit prophylactic stem limited the risk of fracture in the immediate postoperative care for patients with notch depth larger than 5 mm.

As suggested in [58], bone cement plays a crucial role in the implant stabilization and uniform load and strain distributions; thus, the mechanical properties of various bonelike materials have been investigated in the literature. The curing processes of Poly(methyl methacrylate) - PMMA [66], [67], Hydroxyapatite (HA) [68], and Calcium Phosphate (CP) [69], [70] cements were monitored by embedding FBGs in blocks made of such materials. Strain profiles and temperatures were measured over the whole duration of the material shrinkage to check the presence of values out of physiological range, particularly dangerous for tissue necrosis and implant instability. Results in [67] and [69] showed that differences in strain pattern are related to the cement porosity (i.e., the number of voids which occurs after the monomer evaporation), and that a high number cause cement weakness and implant failure. Moreover, according to the porosity level, the immersion of cement specimen in liquid solutions until the saturation allowed the determination of the material expansion coefficients [70].

Once the prosthesis fits perfectly, the evaluation of the mechanism of body movements has been assessed to study the recovery of lost musculoskeletal functions. For instance, FBGs embedded into a carbon fiber reinforced polymer transtibial prosthesis was proposed in [71], [72] to evaluate the recovery of the user's gait. Eight FBGs were placed in a vertical position and nine FBGs in a horizontal position to enable the measurement of vertical strain and mechanical force/strain non-perpendicular to the ground direction, respectively. An additional FBG sensor was placed at the distal end of the prosthesis and used for the temperature compensation. Results of static tests showed a linear response of the proposed system to applied loads with values twice the mass of the volunteer enrolled in the study. Then, three walking tests at three different velocities (i.e., 0.5 m/s, 1.1 m/s, and 2.2 m/s) were performed by attaching the instrumented prosthesis on the knee, showing promising results especially for

the FBGs attached to the regions where the prosthesis stores and releases energy during walking. Such a study, combined with other ones focused on robotic manipulators equipped with FBGs for tactile sensing [73], [74] opens up to future applications of FBGs in bionics. Indeed, FBG-based sensory feedback could enable closed-loop control of the prosthesis, improving its embodiment, amputee's recovery functions, and engagement with the surroundings going beyond the results achieved with MEMS sensors [75], [76].

In the literature, the main orthoses instrumented by FBGs. have been developed in the form of amputee sockets, wheelchairs, fixed platforms, plantar insoles, and orthodontic apparatus. The monitor of pressure at the amputee sockets-stump and skin-wheelchairs interfaces were investigated in studies concerned with the FP7 IASiS projects [77]–[79] whose aim was bringing optical fiber technology in rehabilitation applications, and more recently in [80]–[82]. In all these studies, the sensing element was encapsulated into flexible matrices. Moreover, the influences of the matrix thickness in [79], [80], and the grating embedding depth [80] on the sensor performances have been investigated. For instance, in [80], the amputee sockets-stump interfacial pressures were measured by using an epoxy material sensor pad based on the FBG sensor embedded in a silicone matrix. Results showed that the system with the FBG sensor on the top of the pad encapsulated into the thickest matrix exhibited the highest sensitivity. Foot plantar pressure and ground reaction forces were detected by fixed platforms in [83], [84], and orthotic insoles in [85]–[92] instrumented by single or multiple FBGs. In [89], both shear and plantar pressure were discriminated during gait, using an array of ten FBGs. Other exciting approaches were proposed in [85], and [86] where the two FBGs-based solutions were developed to monitor the ground reaction force: a fixed platform instrumented by five multiplexed FBGs in [91] and a cork-based insole with an array of six FBGs in [92]. Both the proposed solutions were able to monitor vertical ground reaction forces during gait, as well as the body center of mass displacements in static positions. Moreover, corks allowed the gratings thermal isolation. The most recent smart insole was proposed in [90]. The system was completely 3D-printed, and the FBGs were encapsulated into the insole during the printing process with promising during both standing position and walking cycles.

Another important application in orthotics regards the study of dental biomechanics by measuring the properties of teeth and mandible in response to the installation of dental implants and orthodontic apparatus. In dental implants, the main aim is the study of strain-stress patterns on the temporomandibular joint due to the implantation. In all these studies, the sensing elements were directly placed on the outer surface of a mandible equipped with a dental implant [93], [94]. In some cases, strain gauges were used as reference instruments to assess the system capability of measuring a high level of static and dynamic strains, and these measurements were also used to validate FEM [95], [96]. Results in [95] showed a good agreement between the measuring method and FEM when teeth are subjected to symmetrical loads. At the same time, the marked differences during non-symmetric configurations suggested the hardness in replicating the complex dental structure. Moreover, research efforts have also been devoted to study the influence of the sensor positioning on the strain measurement in [97]. Results showed the highest values for sensors positioned in the molar region.

To fix dental implants, often dental cement is required. Thus, FBGs were also used to monitor temperature, strain, and stress built-up during the curing process of gypsum products [98] and dental resin [99]. The most interesting sensing solution was described in [99], where two FBGs in Highly birefringent (HiBi) fiber was employed to monitor the multi-axial stress build-up with promising results. Several studies also reported on the application of FBGs in the presence of dental orthosis involving splints [100] and brackets [101]–[103]. The proposed systems were used to measure temperature, strain patterns, and pressures distributions. Both temperature and force sensing were carried out during the splint positions in [100], showing an increment of both these parameters with small variation in the force values due to the patient self-adjusting. The orthodontic forces applied by a bracket on the dental arch were measured by the custom solutions proposed in [90], and [91]. In [90], an FBG sensor written in a HiBi fiber was bonded on the orthodontic bracket between the orthoses and the incisor outer surface with good ability in detecting longitudinal and transversal forces applied on the teeth, in the range corresponding to clinical applications. Lastly, the influence of grating positions on the strain distribution was investigated in [91], where seven FBGs were placed along three teeth roots and transversally along four teeth apex. As expected, the maximum strain was experienced by the gratings at the cervical position of the molar tooth.

B. MINIMALLY INVASIVE SURGERY

The MIS and the associated tools are becoming increasingly relied upon across the healthcare industry. The term MIS describes all kinds of surgery that minimize injury to the patient with reductions of tissue trauma, pain, and recovery time. Recently, the advent of robotic in MIS imposed an increasing burden on the surgeon's manual dexterity and visual-motor control [104]. However, the use of handheld/robotic tools between the surgeon hand and the tissue, as well as the physical separation in teleoperated surgery limit the haptic feedback to the surgeon with potential tissue trauma or unintentional damage to healthy tissue [102].

To overcome these limitations, FBGs-based tools have been proposed for tasks of tissue manipulation and ablation to restore tactile and temperature sensations fundamental for providing haptic feedback to the surgeon during MIS and robot-assisted MIS [105], [22]. Moreover, to access the surgical target sites along tortuous anatomical paths, several surgical flexible tools have been equipped with FBGs to

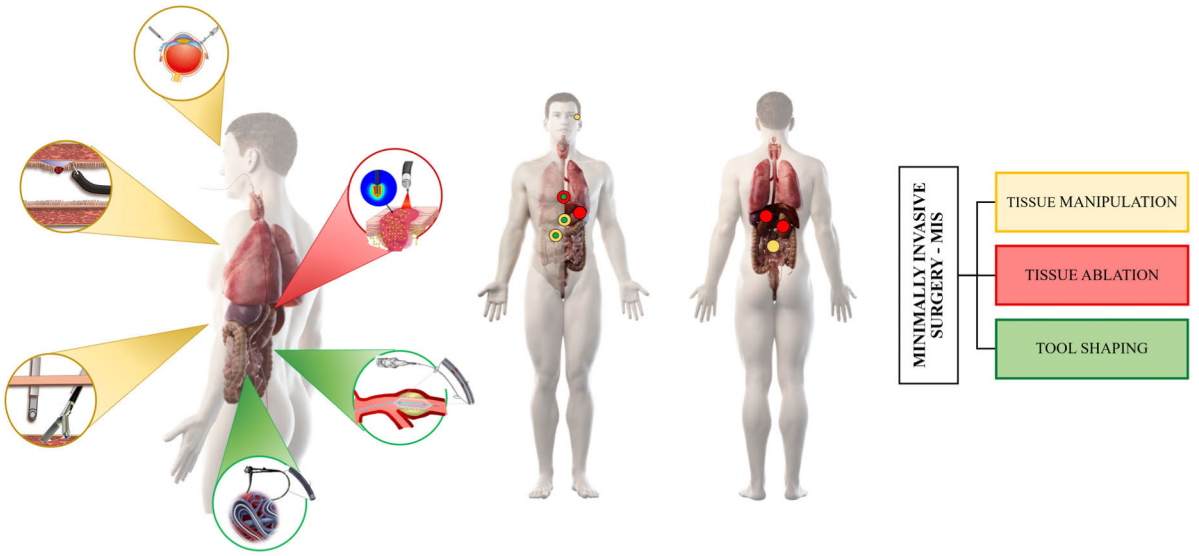

FIGURE 3. Applications in MIS and robot-assisted MIS. Examples of tissue manipulations are highlighted in straw yellow, tissue ablation in red and tool shaping in bright green.

guide and track the tool positioning by monitoring its shape and location [106]. Fig. 3 shows the body parts involved in the following studies grouped into three main categories (Tissue Manipulation, Tissue Ablation, and Tool Shaping). Each category is coded by a different color (i.e., straw yellow, red, and bright green, respectively).

1) TISSUE MANIPULATION

Tissue manipulation includes surgical maneuvers to grasp, clip, suture, and palp outer and inner tissues. These tasks establish tool-tissues interactions to allow unprecedented functionality including, automated robotic responses, recognition of tissue force signatures, ability to minimize tool-to-tissue forces during microsurgery, and potentially improve the safety and efficacy of the surgical procedures. As a result, the surgeon can control the applied forces avoiding any tissue damage and distinguish between hard and soft, healthy, and unhealthy palped tissues [105], [107]. In the literature, several surgical tools as graspers, clippers, needles, and catheters have been instrumented with FBGs for applications of retinal microsurgery, laparoscopy, endoscopy and percutaneous procedures, including epidurals and biopsy [105].

Retinal microsurgery is one of the most technically challenging micron-scale maneuvers performed on delicate tissues [108]. Surgeons need to operate on very small and delicate eye tissue with the magnification of a surgical microscope and fine control of the surgical motion, discharging hand tremor. The proposed solutions ranged from 1 degree-of-freedom (1-DoF) [109] to 2-DoF [110] and 3-DoF [111] tool-tip force sensors based on single and multiple FBGs, with and without temperature compensation. Evaluation experiments with the proposed instruments were conducted on different epiretinal membrane models with manual [112] and handheld robotic control [113]. In [109], the first attempt to develop a 1-DoF FBG-based intraocular force sensor was carried out instrumenting a 25 Gauge ($\sim$ 0.5 mm diameter) micro-pick instrument with a single FBG embedded in a Nitinol wire. Subsequently, by employing three FBGs, the concept was extended to a 2-DoF force-sensing tool with temperature compensation and tests on different epiretinal membrane models with manual [112] and handheld robotic control [113] were performed. In a follow-up work [111], the first sub-millimetric 3-DOF force sensing pick instrument employing four FBGs was proposed to maximize the decoupling between axial and transverse force sensing. Besides assisting with membrane peeling, some FBGs-based tool-tip force sensing instruments were developed to detect puncture forces in retinal vein cannulation. Generally, these instruments employ three longitudinal FBGs for 2-DoF force sensing capabilities attached to a cannulation needle with a distal tip bent at around 45° relatively to tool shaft axis [114]–[116] to ensure sensitivity to puncture forces in the direction of the needle tip. An 80-μm needle tip force sensing cannulation tool was proposed and assessed during the cannulation of synthetic retinal vessel models [114] and cadaver pig eyes [115]. Similarly, in [116], [117], a 70 μm needle tip tool was attached to a handheld robotic device and cannulated vessels in the chorioallantois membranes of chicken embryos. A step forward has been done in [118], where a new control method to actively compensate unintended movements of the operator's hand and to keep the cannulation device securely inside the vein following cannulation was proposed. Experiments in fertilized chicken eggs vasculature, shown 100% success in venous puncture detection and significantly reduced cannula position drift via the stabilization aid of the robotic system [119].

Several studies introduced micro-forceps with integrated FBG-based force sensing [118], [120], [121]. For instance,

in [118], a 3-DoF force sensing motorized forceps was proposed employing an additional sensor to capture the tensile force along the tool axis. Moreover, a nonlinear force computation method was proposed to ensure that grasping does not affect the axial force reading. Validation experiments, including random samples, showed that the method can predict 3-DoF in the axial direction. Lastly, FBG-based force sensors integrated into the tool shaft outside the eye were described in [122]–[124]. This is a highly desired functionality in robot-assisted retinal surgery because the stiffness of the robotic system attenuates the user's perception of the scleral forces with the potential for eye injury. In [122], a tool able to sense the scleral forces in transverse directions, and the location of the sclera contact point on the shaft was developed. This solution allowed a robot control framework based on variable admittance using the sensory information to reduce the scleral interaction forces exceeding a safe level. Furthermore, in [123], a control method was proposed to enable the robot to perform autonomous motions reaching desirable sclera force and/or insertion depth and pre-defined safe trajectories. Moreover, robotic systems, FBG-based force sensing instruments, and a recurrent neural network were combined to develop intelligent assistive solutions to predict excessive force instances and augment the performance of the user [124], [125].

Other surgical applications regard laparoscopic and endoscopic procedures, where FBGs have been extensively used to provide tactile feedbacks inferred from either the exerted forces during surgical tasks or the distal contact force during tissue palpation. Solutions based on one-point and distributed measurements have been proposed using uniform single or multiple FBGs, directly mounted on the tip, in the proximity of the tip or onto a transmission mechanism connected to the tool (e.g., Steward [126], Sarrus [127], and cantilever-beams [128] structures). Moreover, FEMs have been often used to drive the system development in terms of optimized sensor positioning and miniaturized tool dimensions to achieve the best performances. Temperature compensation, axial forces decoupling, bending outward effects, and creep resistance were also evaluated to validate the feasibility of the proposed designs in MIS applications. In [129], a laparoscopic needle driver to measure axial and grasping forces at the grasper tip was proposed. The lower jaw of the grasper was equipped with two FBGs. The FBG sensor used to measure axial strains was embedded in the flexure structure of the jaw, as the deflection of this element during objects pulling induces strain on the grating. The FBG sensor used for measuring grasping force was mounted on the jaw proximally after the flexure segment. This device is an updated version of a previous prototype proposed to overcome some issues related to grasping repeatability and axial sensor hysteresis error in [130]. The novelty lies in the use of a T-shaped grasper made of stainless steel instead of an I-shaped one made of plastic. These features improved the system biocompatibility and sterilizability. The higher rigidity of the steel resulted in a reduction of the system sensitivity in favor of higher repeatability and accuracy with negligible bending and force coupling effects.

However, systems equipped with an FBG sensor directly attached in the proximity to the tip often undergo either limited resolution or operation range. Trade-offs between the force sensing resolution and proximity of the sensors to the tool tip can be optimized by properly choosing the sensor locations. To overcome these issues, some studies proposed the use of FBGs incorporated onto the tool shaft [131] or a transmission mechanism between the end-effector and the joint [128], [132], [133]. For instance, in [131], a 2-DOF needle driver based on four FBGs was developed to be compatible with the Da Vinci Surgical System. Tree robot-assisted MIS tasks were carried out by novice and expert surgeons. Results showed different force profiles according to the level of expertise and improvement in the task execution for both the group thanks to the force feedback. Recently, two interesting solutions based on transmission mechanisms were proposed in [127] and [133]. The same research group focused on two FBG-based systems for grasping and palpation tasks using Steward and Sarrus linkage mechanisms in [133] and [127], respectively. The adopted structures were optimized on the basis of finite element analysis. In both the studies, the rigid kinematic parts of the proposed mechanism were substituted with flexural hinges to provide effective force interaction between tool and tissue and prevent damages to tissues during laparoscopic applications. Moreover, an FBG sensor in a tight suspension configuration was mounted at the flexure's central line. In [133], FEM results suggested the need for an additional cantilever-beam structure to improve the system sensitivity even if sacrificing its axial stiffness and force decoupling. Results in [133] showed an excellent linear response to applied static loads with high sensitivity. A consistent agreement with a commercial force sensor used as a reference was also reported during dynamic loading experiments (the average error between the two kinds of measurement was 0.26 N). Results in [127] showed that in both static and dynamic force loading experiments, excellent consistency was found in terms of simulated and experimental sensitivity and linearity. Then, two simulated cylindrical cancer nodules were buried in the samples at different depth of a silicone phantom and a porcine liver, and the achieved results validated the effectiveness of the proposed sensor to detect tumors from the force distribution map during tissue palpation.

Although over the past two decades, laparoscopic surgery was considered the greatest revolution in MIS and robot-assisted MIS, another surgical revolution for tissue manipulation involved FBGs in natural orifice transluminal endoscopic surgery [134]. In contrast to laparoscopy, no superficial incisions are necessary to reach the target. In the literature, flexible catheters and tubes were equipped with FBGs and inserted through natural cavities [135]. Distal contact force, pressure mapping, and tactile distributions were some of the main measured parameters. For instance, nitinol tubes equipped with two FBGs for detecting the distal

force of tendon-sheath mechanisms in flexible endoscopic robotic surgery were proposed in [136], [137]. The main differences between the two versions are related to the overall length of the nitinol tube (reduced from 6 mm to 3mm) and to the grating length (reduced from 4 mm to 1 mm). Evaluations of force calibration, hysteresis, and temperature compensation were carried out. Results showed linear responses of the two FBGs to force and temperature. Issues related to temperature compensation and creeping effect, as well as signal noise associated to improper glues were fulfilled in [136], and *ex-vivo* and *in-vitro* tests were performed to assess its functionality. Results showed a stable response with good linearity within the range of 0.1 N - 0.5 N with a percentage error of 4.19% between the measured and the theoretically estimated values.

An interesting application of two FBGs arrays with thirty-two gratings each, for pressure mapping in gastroscopy was proposed in [138]. A flexible catheter was inserted through the nasal hole with a sensing length covering the path from the pharynx to the stomach for monitoring the gastrointestinal mobility. Firstly, controlled *in-vivo* clinical trials were carried out to directly compared the system performance with a commercially available solid-state manometry catheter showing a substantially equivalent response. Then, a volunteer was intubated and asked to perform controlled swallows. Results demonstrate the ability of the FBGs-based catheter to record peristalsis running from pharynx to stomach by measuring muscle contraction (pressure increments) and retraction (pressure decrements). Abnormal values can allow measuring early symptoms of diseases related to the upper digestive apparatus. Another FBG-based system suitable to work inside the digestive apparatus was proposed in [139]. An endoscopic instrument was developed for palpation of the inner colonic wall for future applications in colorectal cancer screening. The device was equipped with three silicone-encapsulated FBGs. A FEM guided the system development demonstrating the capability of the proposed tool to measure contact forces along its axis with a linear response between strain and applied forces.

Other percutaneous procedures for tissue manipulation involved FBGs-based needles for biopsies and epidural punctures [140]–[142]. Solutions for tissue-tool tip force sensing have been proposed in the form of needle equipped with FBGs. In [140], an 18 Gauge needle stylet was equipped with three optical fiber embedding four FBGs each. The needle was mechanically connected to a device with a pen-like knob grasped by the users, and information of tool-tissue contact was rendered via a haptic display that uses ultrasonic motors to convey directional cues to users. An amount of twenty puncture trials were performed by each of the ten subjects involved in the study. Results showed that subjects could easily determine the direction in which haptic feedback was guiding them, improving their task performance. Lastly, an optical guidance system for epidural space identification was proposed in [141]. An FBG sensor was placed inside the lumen of an 18 Gauge epidural needle and tested on a lumbar phantom used to train clinical procedures for epidural space identification. Intentionally wrong punctures without achieving the epidural space were also performed. Results showed the system capability of discriminating the most significant tissue interfaces from the detection of the pressure state experienced by the needle tip during the penetration inside the phantom model. Moreover, the correct and wrong punctures were clearly distinguished.

2) TISSUE ABLATION

Another important application of MIS is the cancer removal through tissue thermal ablation. Localized measurement of temperature distributions inside the organs may improve the clinical outcomes reducing the probability of damaging surrounding healthy tissue. Tissue ablation by thermal treatments (e.g., laser ablation, radiofrequency ablation, microwave ablation, and cryoablation) have an immense potential for the removal of cancer and have already gained broad clinical acceptance [143]. The main advantages are related to their minimal invasiveness since these treatments can be performed either via a percutaneous insertion of a small needle-like applicator or through a natural orifice under endoscopic ultrasound guidance. Thermal treatments involve the use of different types of energy to induce a cytotoxic temperature increment in the target organ in order to destroy all the tumors with an additional safety margin while sparing the surrounding healthy tissue. Although these techniques have been performed for decades, there are some open challenges. The high temperatures induced to destroy tumors, inevitably damage healthy cells. In addition, the difficulties to accurately monitor in real-time the effects of the treatment can cause either an incomplete tumor removal or the damage of surrounding healthy structure. FBGs have immense potential for improving the clinical outcome in this field since the knowledge of temperature during the treatment can be beneficial to target the thermal damage to tumor cells minimizing the harm of healthy tissues [144], [145]. The possibility to resolve temperature along with the fiber by fabricating FBG arrays facilitates the 3D reconstruction of tissue temperature. This unique characteristic makes FBGs better than other temperature sensors (e.g., thermocouples, thermistors) for this application. In 1997, first attempts to monitor temperature during thermal ablation by FBGs were presented in [146]. In the last decades, FBGs usage in this field has grown tremendously, and these sensors have been applied in phantoms and during the treatments of different organs (e.g., liver, bone, kidney, pancreas, biliary tree) in animal models (*ex-vivo* and *in-vivo*) and in clinical trials [146]–[154]. During the first attempts, the majority of the studies have been performed by using one or more fiber optics embedding a single FBG sensor, while recent investigations have employed arrays of FBGs to perform high resolved measurements and to reconstruct the whole map of temperature within the organ. Recently, studies have proposed highly dense FBGs with spatial resolution better than 1 mm with ten or more FBGs embedded within a single fiber. For instance, recently,

a configuration using an array of twenty-five FBGs with a grating length of 0.9 mm was proposed in [155]. Regarding other performances of these sensors, it is worth noting that they can measure temperature with accuracy in the order of 0.1 °C, with short response time, and data can be collected at sampling frequency higher than 1 kHz [22], [151], [155]. Other advantages are related to the absence of artifact due to the direct absorption of the energy delivered to perform the treatment, while this problem can significantly affect different types of sensors [156]–[158]. An important advantage is that these sensors can be used in Computed Tomography (TC) and MR room. This can be crucial since several thermal treatments are performed under either CT or MR guidance. In addition, this feature makes FBGs an optimal tool for assessing the performance of new non-invasive protocols for monitoring temperature maps during thermal treatments by CT or MR images (e.g., CT thermometry and MR thermometry [159], [160]). A potential problem can be related to the cross-sensitivity to strain, especially during *in-vivo* experiments. In this scenario, movements caused by the respiratory activity of the patients can strain the sensors causing measurement errors. This concern involves not only applications during lungs' treatments, but all the organs which experience movements during respirations (e.g., liver, pancreas, and kidney). Experiments have shown measurement error up to some °C, but they can be minimized by filtering the recorded data [151]. Recently, CFBGs have been applied to this field to estimate the thermal gradient, which is particularly significant close to the applicator used to deliver the energy during the treatment [15]. The recent developments of highly dense FBGs allowing measurements with high resolution could discourage future use of CFBGs in this application, also considering the complexity of the data analysis to retrieve information from their spectrum.

3) TOOL SHAPING

For the correct manipulation of surgical tools inside the patient's body, it is essential to dynamically track their position and shape during a surgical procedure. Despite the availability of commercial FBGs-based shape sensors certified EN60601 (a series of standards for the safety and the effectiveness of medical electrical equipment) [161], the 3D real-time shape reconstruction is still challenging. Indeed, the complex morphologies of the targeted sites and the tortuous path access under constrained spaces require high embedding capability of the sensing system and inherent tool deformability. To overcome these issues, optical fiber technology has gained attention for curvature estimation and shape reconstruction. The main configurations of FBGs-based shape sensors can be grouped into multiple single-core fibers, epoxy-molded or fastener to a support, and multicore fibers (MCFs), having several cores integrated into a single fiber. The most widely used configurations for shape sensing are: triangular with three outer cores [162], [163], square with four outer cores [164], [165], and hexagonal with one central core and six outer core [163] (typical configuration for MCFs). The more cores are exploited, the higher is the accuracy of the shape sensor at the equal value of core spacing (core-to-core distance) [166]. Besides, some studies investigated the multi-sensitive capability of shape sensors for simultaneously detecting the interaction forces between the instrument and the surrounding environment, while reconstructing shape [167], [168]. Needles, catheters, endoscopes, and continuum robots for MIS and robot-assisted MIS applications (e.g., in neurosurgery, otolaryngology, biopsy, colonoscopy, and intravascular surgery) have been equipped with FBGs, showing enormous potentialities in tool shaping. Among the instrumented tools, better performances have been found in the shape reconstruction of systems which undergo small deformations (e.g., steerable needle for biopsy and ablation). Indeed, their inherent higher stiffness in comparison to catheters and endoscopes induced a perfect strain transmission to the attached FBGs.

Referring to multiple single-core fibers, the triangular configuration has been the most exploited in medical applications, since it can be interrogated using only three channels of the interrogation unit and ensures a simpler assembly than the other configurations. Furthermore, when employing a central core, such configuration allows twist angles detection in addition to temperature compensation, axial strain removal, and curvature sensing [105]. For instance, in [162] and [163], a surgical needle was equipped with a triplet of single-core optical fibers in a triangular configuration. Each fiber embedded four FBGs glued along the shaft grooves for shape sensing during a biopsy. Results in free space and gelatin phantom insertion showed maximum errors in needle shape reconstruction and tip positioning (about 2.23 mm and 1.91 mm in free space, and 0.79 mm and 0.57 mm, in gelatin), higher in out-of-plane deflections than in in-plane ones. Improvements in target accuracy and precision of the proposed system were reached by combining a robot-assisted needle steering method with FBGs-based shaping feedback [169]. Attempts have also been made toward the shape sensing of endoscopes and catheters. Their length and flexibility higher than the ones of needles require more FBGs to provide useful and accurate curvature information. Moreover, research efforts have been dedicated to the implementation of shape sensors in endoscopes. For instance in [164] and [165], where a four single core fibers, each consisted of five FBGs and in a square configuration, was proposed. Results showed the system capability of reconstructing the tool shape but with large errors during *in-vivo* tests [164]. This configuration allows the temperature compensation and curvature profile measurement but suffers from low resolution in twist angle detection [165]. Recently, a step forward to the accuracy improvement of shape reconstruction has been done exploiting MCFs arranged in a hexagonal configuration, as reported in [170]. Such a system resulted in a valid alternative to fluoroscopy for endovascular navigation. The shape sensor was obtained using three of the seven cores of the MCFs, inscribing thirty-eight multiplexed FBGs each, to sense

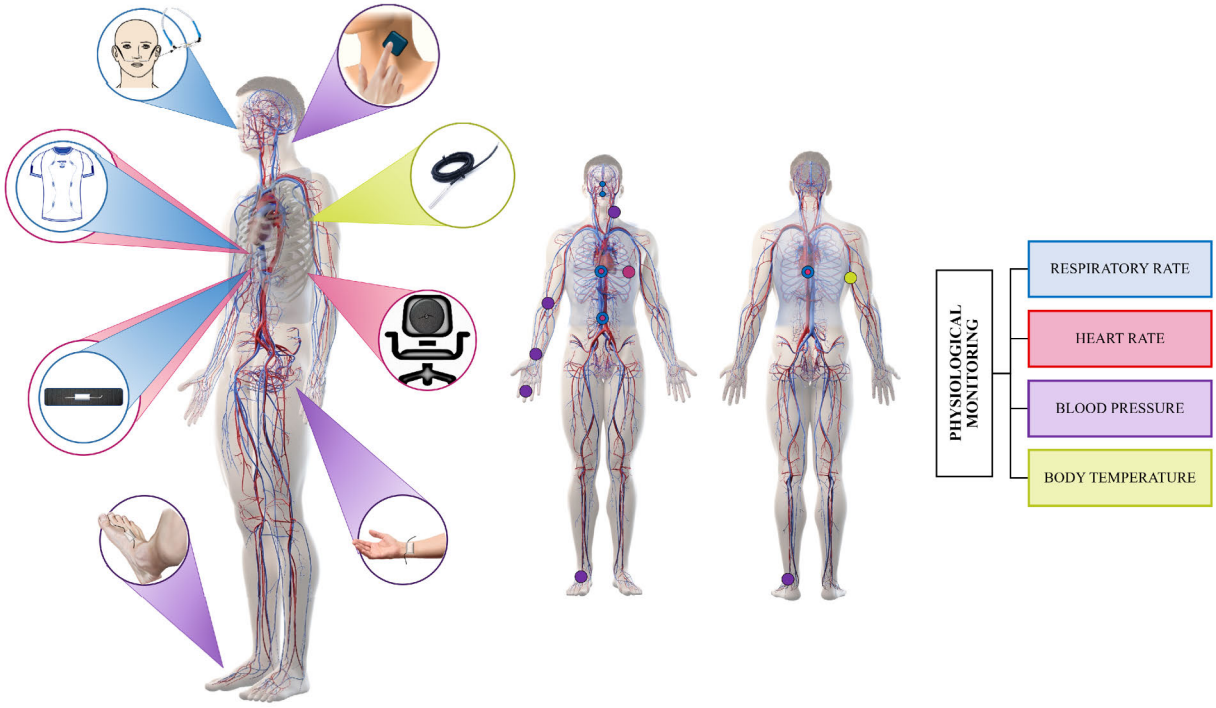

FIGURE 4. Applications in physiological monitoring. Examples of systems for monitoring RR are highlighted in light blue, for HR in light red, for BP in purple and for BT in acid green.

curvature and shape from the strain detected by the gratings. Results showed high accuracy in the 3D shape reconstruction over the whole sensing length (380 mm).

C. PHYSIOLOGICAL MONITORING

The monitoring of physiological parameters is at the cornerstone of medicine and surgery since it is a relatively non-invasive measure of human health. The baseline indicators of a patient's health status are often known as vital signs [171]. This section is devoted to describing the FBG-based systems used to detect vital signs routinely checked by healthcare providers: respiratory rate (RR), heart rate (HR), blood pressure (BP), and body temperature (BT). Fig. 4 shows the body parts involved in the following studies grouped into four main categories (i.e., Respiratory Rate, Heart Rate, Blood Pressure, and Body Temperature). Each category is coded by a different color (i.e., light blue, light red, purple, and acid green, respectively).

1) RESPIRATORY RATE

The RR has been extensively monitored by using FBGs-based technologies in clinical (e.g., respiratory rehabilitation, and MR examination) and sports settings (e.g., cycling and archery) [172]. The majority exploited the grating intrinsic strain sensitivity for developing wearable and non-wearable systems able to monitor RR from the respiratory-induced chest wall deformations. In this kind of application, FBGs have been either bare or housed into passive flexible matrices, bonded on textiles (e.g., elastic bands, and stretchable T-shirts) or on synthetic surfaces the body skin comes into contact with (e.g., cushions, wheelchairs, flatbeds [173], [174]). Spirometers, flowmeters, and MoCap systems have been often used as benchmarks [175]–[178]. The first study concerning the monitoring of RR by thoracic cage deformations was described in [179]. An FBG sensor was embedded in an elastic band to hold it in place during breathing. Good signal-to-noise ratio, not fully linear response to strain and capability of triggering external devices for artificial ventilation, was demonstrated. FBGs used to instrument wearable system were also proposed in [180]–[182], in the framework of the financed OFSETH FP6 EU project. Both thoracic and abdominal movements were detected by smart elastic bands. One band was instrumented by a single FBG in a coiled-layout fiber. Once the strain sensitivity and fatigue strength have been studied, the system assessment was performed on healthy adults and using a simulator inside the MR scan. The capability of measuring strain elongation up to 3% and to be a golden solution for MR vital signs monitoring was demonstrated. Smart T-shirts based on a different number of FBGs (from two up to twelve gratings) have been proposed as innovative technologies enabling unobtrusive respiratory monitoring in terms of RR, respiratory (TR), inspiratory (TI) and expiratory (TE) periods, tidal (Vt) and compartmental (Vc) respiratory volumes in [177], [178], [183]. Indeed, a high number of gratings allows investigating the behavior of different chest

compartments. For the first time, MoCap system was used to drive both the system fabrication and assessment. Tests in standing and supine positions, as well as during MR scan and cycling, were carried out to investigate the system response to different working conditions. The promising results showed that the system performances increased with the number of gratings, their location, and orientation (for instance, percentage errors in RR estimation $\leq$ 0.38% [183] rather than 1.59% [178] and 1.14% [177]). Moreover, the smart textile based on twelve FBGs, a half located in specific positions on the front of the cage and a half on the backside, showed high accuracy in estimating breath-by-breath TR, TI and TE values (for instance TR bias of 0.001 s rather than 0.14 s [178] and 0.04 s [177]) with good capability of monitoring Vt after a pre-calibration (bias of 0.09 L). Such a prototype was also involved in studies where influences of sex and sensor positioning have been considered for driving further optimization in terms of the number of FBGs, robustness, and more adaptability to different body shape [184].

In this regard, two different branches of research have been proposed: *i*) the sensorization of synthetic surfaces in contact with the skin (e.g., cushions, wheelchairs, flatbeds [173], [174]), and *ii)* the rise of flexible wearable sensors based on FBGs, high compliant to the skin [185]–[187].

Some examples belonging to the first branch are FBGs taped on a cushion [173] and a plexiglass board [188], placed between the backside of the chest and the backrest of the seat or the MR flatbed, respectively. Results showed good performance in measuring dynamic strains caused by the breathing (in both cases, percentage errors $<$12%).

Regarding the second branch, an amount of novelty has been brought by studies based on flexible sensors to be comfortably worn by the subject. In these works, often a metrological characterization is firstly required to find out the sensor sensitivity to strain, and other parameters (e.g., temperature and relative humidity) since the properties of the 3D matrix influence the FBG response. For instance, in [187], a rectangular-shaped flexible sensor based on FBG technology was calibrated to retrieve static and dynamic metrological characteristics showing strain sensitivity one order of magnitude bigger than the temperature ones, negligible relative humidity-induced contributions, and acceptable hysteresis errors. Then, the proposed sensor was used to instrument two elastic bands for monitoring mean and breath-by-breath RR values from the thorax and abdomen movements during tests in lab and out-of-lab (i.e., during simulated archery races) [176].

A different approach for the RR monitoring involved the measurement of nasal/oral airflow. Techniques for a direct measure of the respiratory airflow or based on different thermo-hygrometric conditions between inspiration and expiration have been proposed. The main difference between these two techniques is related to the presence of active polymer coatings for the grating functionalization. This configuration allows variations in the surroundings (i.e., in the content of water vapor and so in relative humidity, and temperature) to activate the coating volumetric or refractive index changes responsible for FBG wavelength shifts and coupling intensity variations. This configuration allows variations in the surroundings (i.e., in the content of water vapor and so in relative humidity, and temperature) to activate the coating volumetric or refractive index changes responsible for FBG wavelength shifts and coupling intensity variations.

Focusing on the direct monitoring of respiratory airflows, both bare and metal-coated FBGs have been used to develop flowmeters (e.g., orifice meters, and hot wire anemometers) and spirometers. Cantilever-based mechanisms and external energy sources (e.g., laser) have been often required for the transduction of the airflow into FBG output changes. For instance, in [189], an isosceles triangle cantilever with a couple of FBGs at either side was pushed/pulled by the flow force transmitted on it. The cantilever bending caused grating tensions/compressions, showing a non-linear relation between wavelength shifts and measured flowrates with a high strain sensitivity. Another cantilever-based approach was proposed in [190], where a spirometer based on FBG technology was proposed for pulmonary function tests. The FBG sensor was glued lengthwise along a cantilever beam mounted transversely to the upper section of an aluminum plate. During inspiration/expiration, the cantilever was pushed/pulled by the plate swiveling, and in turn, the FBG sensor was tensioned/compressed. The comparison between some crucial respiratory parameters (i.e., forced expiratory volume in the first second, FEV1, forced vital capacity, FVC, and peak expiratory flow, PEF) obtained by the FBG outputs and the reference one measured by a commercial spirometer showed promising results.

Research efforts have also been done in the use of metal-coated FBGs to develop hot wire anemometers, where an external source of energy has been often used to ensure the sensing element thermal equilibrium. Recently, examples of this kind of solution were described in [191], [192], where graphene and silver layers were used as coatings, respectively. Their measurement principle is underpinned by the metallic layers, which absorb the power of pumping light. Usually, an external source heats the metallic layer causing a red shift of the coated FBG sensor. When the airflow hits the sensing element, part of the heat is taken away from the layer, and the FBG undergoes a blue shift. All these works showed an effective improvement of the system flowrates sensitivity thanks to the metallic layer, with a non-linear relationship between FBG wavelength shifts and measured flowrates.

As previously described, changes in airflow thermo-hygrometric conditions can also be exploited for RR monitoring. Few studies proposed devices with bare FBGs to estimate RR by detecting temperature changes between inhaled and exhaled airs [193], [194]. The most used solutions are based on the FBG functionalization for relative humidity sensing [195]. To accomplish this aim, several coatings have been exploited. Among others, synthetic and natural

polymers (e.g., PVA, PMMA, and Agar) and nanostructured films of Graphene oxide (GO) and Polycyclic aromatic hydrocarbon/Silica nanoparticles (PAH/SiO_2). The matrix thickness and coating concentration have been investigated as influencing factors of the relative humidity sensitivity of functionalized FBGs suggesting higher sensitivity and response times for thicker matrices and higher polymer concentration [196].

These solutions allow RR monitoring from the oral or nasal airflow in the form of needle-like probes and temporary wearable devices (e.g., face masks and plates below the nostrils), with uniform FBGs and TFBGs working in reflection or in transmission [197], [198]. An FBG sensor inserted in a metallic needle and coated by agar was proposed in [175], [199], [200] for RR monitoring during both mechanical ventilation and human breathing. The measured RR values were compared with the ones set on the mechanical ventilator and measured by using a commercial spirometer in [199], [200], and [175], respectively, showing promising results (percentage error $<3\%$).

Amon temporary wearable devices, a respiratory mask instrumented by an FBG sensor coated by GO was used in [197] and by 23 PAH/SiO_2 layers in [201]. Both the devices showed a high capability of monitoring RR but only the one in [201] was tested on humans. A more comfortable solution was recently proposed by [202], where a completely MR-compatible plate made of PVC was instrumented by an agar-coated FBG sensor encapsulated into a Dragon Skin^{TM}matrix. The assessment was carried out on six volunteers during slow, normal, and fast breathing, placing the plate below the nostrils. Promising results were testified by values of absolute percentage errors $\leq 2.29\%$.

2) HEART RATE

The HR has been monitored simultaneously to RR by most of sensing FBG-based solutions previously described to measure chest displacements [173], [183], [185]–[187]. Indeed, the mechanical activity of the heart causes vibrations smaller and faster than the respiratory ones on the chest surface. The graphical representation of the heartbeat-induced displacements is known as seismocardiogram (SCG) when measured as vibrations on the chest, and ballistocardiogram (BCG) when referred to the ballistic forces generated by the heart and measured at the center of mass of the human body. FBGs are very suitable for non-invasive cardiac monitoring since they are small and light, highly sensitive to strain, with long-term stability and proper frequency response. These features allow the recording of cardiac-induced displacements, typically ranging from 0.2 mm to 0.5 mm and frequency components, mainly ranging from 0.6 Hz and 40 Hz [203]. The majority of the proposed studies investigated the cardiorespiratory monitoring describing wearable and non-wearable solutions made of polymers and composite materials such as Polydimethylsiloxane - PDMS [186], PVC [185], [204], Dragon Skin^{TM}20 [187], Plexiglass [205], Fiberglass [206] and reinforced carbon fiber (CFRP) [174]. Electrocardiogram (ECG) and photoplethysmography (PPG) have been often used as benchmarks [205]. Despite the use of different measurement principles and various casing materials, all the studies agreed with each other: the proposed systems show more accuracy in the estimation of RR than HR values. This finding is justified by the smaller amplitude of the signal related to the heart activity than the one due to respiration, by the need of more sophisticated filtering stages required to extract the cardiac contributions masked by the respiratory one, and by the lack of standardized fiducial measuring points for the SCG detection. Such harnesses are still limiting the clinical use of SCG/BCG signals for HR monitoring.

Recently, a first effort in the definition of fiducial points has been done in [176], [187] where an elastic based instrumented by a flexible sensor based on a single FBG was positioned on three measurement sites (i.e., xiphoid process, umbilicus and below the left mammilla) of 3 volunteers to investigate the site influence on the signal amplitudes. Significant differences were found during both inter- and intra-volunteer analysis, suggesting the influence of anthropometry and sensor pre-stretching. However, the low values of standard deviation measured during each test indicated the high repeatability of the system once worn and the capability of measuring HR. A step forward has been done in [164], where HR was measured by two nominally identic FBGs, one sensor worn on the xiphoid process and the other one above the umbilicus of 9 volunteers. The FBG sensor at the xiphoid process resulted more accurate than the one above the umbilicus in estimating HR values when compared to the reference one, both in terms of mean and beat-by-beat values (e.g., mean absolute percentage errors around $\sim 5.74\%$).

Other exciting solutions for potential SCG clinical applications have exploited the FBG MR-compatibility. In [205] and [206], HR during the MR scan was measured, placing the sensor in contact with the backside of enrolled volunteers and the thorax (i.e., in the form of a wearable system), respectively. Despite the strong electromagnetic field generated inside the MR scanner, the signal propagated in the fiber was not distorted, and a good agreement (percentage errors $< 7\%$ for both the proposed systems) was found between mean and beat-by-beat HR values measured by the FBG-based system and the reference instrument. The same system in [205], was used to instrument a chair and a footplate. Results of 3 volunteers showed differences always lower than 2.68 bpm between HR values obtained by the FBG and the ECG sensors. Similar approaches were proposed in [174] and [204]. In [174], a smart bed equipped with 12 FBG in a single fiber was proposed. Results showed that the HR detected by the smart bed was very close to the one measured by a pulse oximeter. Lastly, in [204], a conic-shaped device was instrumented by an FBG sensor and used to measure HR when positioned in contact with the left upper thorax of five volunteers. A comparison between mean HR values measured by the FBG sensors and a digital oscilloscope showed good agreement.

3) BLOOD PRESSURE

The BP calculated from the pulse wave using FBGs is one of the most challenging measuring techniques concerning vital signs monitoring. Indeed, a low-pass filtering stage (e.g., 0.5Hz-5Hz), the identification of each single pulse wave, the signal normalization along y-axis and standardization along the x-axis, and a calibration curve built using partial least squares regression analysis are necessary before being able to calculate BP. [207]

Usually, when the heart beats, the pulse wave moves through the circulatory system. In the literature, several FBGs-based solutions were proposed to perform the pulse wave analysis (PWA), detecting the arterial pulse at different peripherical pulsatile sites. The PWA has been extensively used for monitoring BP (and the pulse rate, PR) starting from the peaks in the pulse wave patterns. The advantage of PWA also relies on monitoring pulse variability in terms of pulse transit time (PTT) to retrieve an estimation of the arterial stiffness and of the waveform and to improve the quantification of the systolic load on the heart and other central organs [208]. Sphygmomanometers placed on the arm/wrist, pulse oximeters on the finger, and stethoscopes have been often used as benchmarks. Systems based on FBGs for BP monitoring have been fabricated to be directly attached to the skin [207], encapsulated into wearables [209], [210], or embedded into probes in contact to the skin surface [211]–[213]. The pulse wave has been detected on several body parts (i.e., temple, finger, ankle, neck, foot, elbow and wrist [209], [210], [214]–[217]), at the level of the peripherical pulsatile sites (i.e., brachial, carotid, radial, ulnar and tibial arteries). In [207], [218], an FBG sensor was used for BP monitoring. It was taped perpendicularly to the direction of the blood flow in the radial artery of the right wrist. A sphygmomanometer around the left upper arm was used as a reference system. Moreover, influences of individual differences, measurement site height, and assumed postures on the accuracy of the BP monitoring have been investigated in [207], [218]. Tests were carried out on participants included elderly and young subjects in supine posture in [207] and in supine, sitting, and standing positions with increasing differences in height between the FBG sensor and the reference instrument in [218]. Results showed the good capability of the proposed sensor to calculated BP in several postures at fixed heights (error < 4 mmHg) with a reduction of accuracy according to individual differences and height (errors < 6 mmHg in both cases).

Attempts have also been devoted to the employment of wearable solutions for the BP monitoring. They have been developed in the form of skin-like systems [209], and hollow boxes [210], [219], [220] with a flexible diaphragm. The most recent solution has been proposed in [210], where an FBG-based hollow tube was developed to detect pulse waves from the volumetric changes of the finger. The results of eighteen volunteers showed the capability of the proposed device to monitor BP, PR, and PTT, using an electronic stethoscope as reference. Moreover, repeatable morphologies between followed pulse have been demonstrated. Lastly, among optomechanical probes based on FBGs, two studies proposed spring- and lever- based mechanisms to improve the systems' sensitivity to the small strains caused by the pulse wave [211], [213]. Both the works showed highly performant solutions for BP monitoring. Indeed, such mechanisms improved the strain sensitivity around ten and twenty times in comparison to the ones obtained without transmission elements.

4) BODY TEMPERATURE

The BT has been monitored in some studies reported on FBGs-based systems. Needle-based systems and wearables have been proposed. Commercial thermometers have been often used as benchmarks. In [221], a polymer packaging was used to improve sensitivity of bare FBGs. In particular, an unsaturated polymer resin encapsulating the grating allowed an increment of temperature sensitivity around 15 times higher than the bare one. Then, five prototypes of the proposed sensor were embedded into an upper body intelligent cloth, on the right and left chest and armpit, and on the upper back. A weighted FEM was proposed to obtain the final BT from the five sensors placed on the upper body. Indeed, the contribution of each body part to the final BT values is different and should be weighed. A good agreement was found between the last BT values measured by the proposed system and the ones measured by a medical mercury thermometer. A Teflon-based capillary structure was proposed in [222]. First, the capillary was filled with epoxy resin. Then, tests were carried out by placing the proposed system and a mercury thermometer into a water bath at identical positions, when temperature ranges from 35 °C to 45 °C. A nonlinear input-output relationship was found presumably related to the resin solidification process. Thus, to improve the system performance, another structure was proposed by fixing the FBG sensor only at two endpoints. Results showed a linear response with a temperature sensitivity 23 times higher than the ones of a bare FBG sensor. Lastly, a prototypal FBG probe consisting of a hypodermic needle has been recently proposed in [223] and subjected to cyclic sterilization processes. The aim was the investigation of the influence of such a process on the FBG-based probe performances when compared to a commercial thermistor. Results showed that the optical probe was not harmed from thermal stress cyclically induced by the sterilization while the thermistor was affected. Moreover, the temperature sensitivity of the FBG-based needle showed no significant changes with the accumulation of sterilization cycles (up to 250), and the standard deviation remained low and stable over the cycles as compared to those determinates by the commercial system. These findings are considered very promising for clinical practice.

D. MEDICAL BIOSENSING

The need for even more accurate diagnosis and personalized medicine is leading to a growing understanding of disease pathological pathways through the detection of biomarkers.

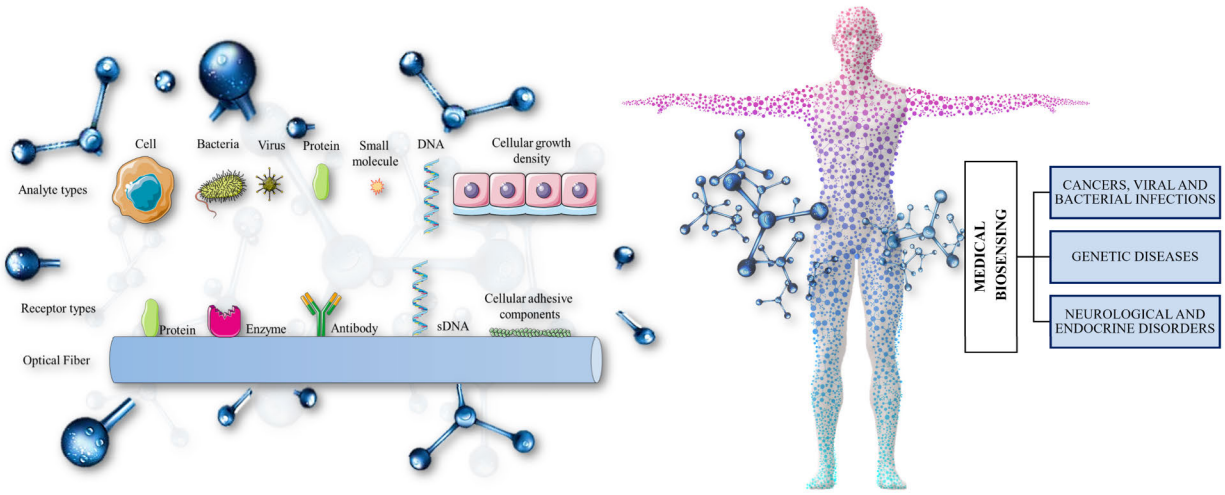

FIGURE 5. Applications in medical biosensing. Examples of the main binding typologies are highlighted.

Biomarkers are considered efficacious indicators for several pathologies such as cancers, neurodegenerative disorders, and cardiovascular disease [224]. For this reason, researchers have invested a lot of effort in the field of medical biosensing with the aims of promptly assessing the stage of the disease and designing the most effective treatments tailoring to the patients' individual needs [224], [225]. A biosensor is a compact device that incorporates a high-affinity biological receptor (e.g., enzymes, aptamers, cells, and antibodies) for the recognition of a specific analyte (e.g., proteins, DNA/RNA sequences, virus, and bacteria) [226]. Among others, medical biosensing based on optical fiber gratings presents good performances in detecting biological components since the recognition of the analyte is transduced into a measured optical signal with high sensitivity, immune to external disturbance, stable and with high signal-to-noise ratio [225]. Although TFBG is the principal grating configuration used in optical biosensing, also EFBGs have attracted recent interest as biosensors [20]. However, some hurdles are still limiting their use.

In biosensing applications, all the proposed sensing solutions should be able to detect changes in the surrounding refractive index caused by the biochemical receptor-analyte reaction. Thus, the first step forwards the fabrication of EFBGs-based biosensors is the partial or full exposition of the core-inscribed sensing part to the surrounding medium obtained by etching, polishing, or tapering the fiber [225]. Usually, the chemical etching has been performed before the grating functionalization to improve the biosensors' surrounding refractive index sensitivity. Unfortunately, although a smaller diameter results in a higher sensitivity to refractive index, an improvement in the fiber fragility during the functionalization steps is observed. Some studies have focused on the influence of EFBG diameters on the system performance to find out a good trade-off between refractive index sensitivity and robustness [227], but challenges still exist. Otherwise, TFBGs can be directly used for biosensing purposes exploiting their intrinsic sensitivity to surrounding refractive index changes.

The most widespread optical configuration for medical biosensing is represented by the surface plasmon resonance (SPR) based biosensors. Numerous studies reported on pure and localized SPR excitations obtained by coating the grating with noble metal films and nanoparticles (e.g., gold and silver). Moreover, silane chemistry has been often performed as an additional biofunctionalization strategy to allow an appropriate immobilization of bio-receptors on the sensor surface. Lastly, the blocking of the uncovered sections to avoid non-specific analytic bindings and additional depositing of nanoparticles (e.g., gold, and GO) have been proposed to improve the sensor selectivity and sensitivity [228]–[230].

The choice of reagents depends on the final target applications. EFBGs- and TFBGs- based biosensors have been used for detecting metabolic pathways, cellular growth and proliferation, proteins, bacteria, as well as viruses to allow diseases and disorders detention, drug testing, and cellular regeneration. Most of the proposed detection technologies have not required fine labeling procedures, and the binding process could be assessed and monitored in real-time. Confocal and fluorescence microscopy-based approaches have been used to provide the assessment of the effectiveness in modifying the fiber surface [231], [232]. Biosensors based on FBG technology have been extensively used for applications in medical diagnostics, ranging from the detection of cancers, viruses, and bacterial infections to cardiovascular, neurological, and endocrine disorders and diseases. According to the biological reagent in charge of capturing the analyte, the proposed EFBG/TFBG-based biosensors can be grouped into antibody-, nucleic acids-, enzyme- and whole cell-based biosensors. The most popular biosensing technique for pathologies diagnosis is based on the immobilization of a bio-receptor (e.g., antibody, aptamer) on the fiber surface to capture a specific biological target (e.g., protein, virus, bacteria, whole-cell, and small molecules) [233]. Fig. 5 shows

the main diagnostic areas targeted by the following studies grouped into three main categories (i.e., Cancers Viral and Bacterial Infections, Genetic Diseases, and Neurodegenerative and Endocrine Disorders).

1) CANCERS, VIRAL AND BACTERIAL INFECTIONS

Systems for a prompt diagnosis of cancers, and infections caused by viruses, and bacteria have been proposed starting from the EFBG/TFBG detection of changes in refractive index due to the antibody-antigens reaction binding. In [228], the diagnosis of lung cancer in the distal bronchial tree was proposed. The group manufactured a minimally invasive gold film-coated SPR-TFBG sensor. The biosensor was embedded inside a catheter and designed to detect a cancer cell biomarker (i.e., Cytokeratin, CK 17) by the surface immobilization of a specific antibody (i.e., anti-CK17). *Ex-vivo* studies on freshly resected human lobectomies showed that the device detected the biomarker and hence distinguished healthy samples from tumoral ones. Moreover, additional information about the tissue stiffness allowed the right positioning of the catheter. Recently, nucleic acid aptamers (DNA or RNA) have been emerged as attractive alternatives to antibodies, leading to the development of nucleic acids-based biosensors based on FBGs. Cancer biomarkers were detected by DNA-based biosensors in [228]. A specific DNA aptamer (i.e., MAMA2) was immobilized on the fiber surface (50 nm gold film-based SPR-TFBG sensor) for the detection from the tissue surface of mammaglobin proteins, expression of circulating human breast cancer cells. Moreover, additional gold nanoparticles were used as amplifier label of the biosensor response. Results showed the capability of detecting a low concentration of cancer cells (10cells/ml) with a good specificity as compared to other control cell lines.

Other studies have focused on the diagnosis of cancers and inflammatory processes from the detection of the cell growth density in response to cancer biomarkers drugs and other stimuli using whole cell-based biosensors. Among others, in [234] and [235], the detection of the epithelial growth factor receptor (EGFR) was performed. The EGFR is an important biomarker which is over-expressed by numerous cancer cells [236]. In [234] and [235], the functionalization of the fiber surface with specific monoclonal antibodies was performed to quantify extracellular membranes receptors in native human epithelial cells.

In both the studies, the sensor architecture lay on a gold-coated SPR-TFBG with monoclonal mouse immunoglobulin G antibody (anti-EGFR) immobilized using Dojindo's carboxylic acid. The interaction between the proposed immunosensor and EGFRs (intact and with an overexpressed receptor) was investigated by measuring changes in transmission spectrum amplitude and wavelength as cellular binding events occurred. Specific bindings of cells were detected for concentration $\geq 3.0 \cdot 10^6$ cell/ml with linear binding relation over time.

In the field of cell growth density, another application has focused on the investigation of drugs and microenvironments- cell interactions in cell culture equipment. The effect of trypsin, serum, and sodium azide on the NIH-3T3 fibroblast cells response was studied by using a gold-coated SPR TFBG [237]. Results showed that such stimuli induced detachment of cells from the sensor surface, serum uptake, and cellular metabolism inhibition, respectively. The resulting signal indicated a regeneration capability under repetitive stimuli and the possibility of detecting biofilm formation and drugs on the fiber surface.

2) GENETIC DISEASES

Another innovative field of application in medical diagnostics relies on the detection of genetic diseases performed by biosensors based on DNA hybridization [231], [232]. Indeed, the discovery of imperfect matches of DNA sequences is the leading cause of specific genetic mutations. Although innovative efforts have been assayed towards the development of such biosensors, the development of high performant sensing solutions is still challenging. In [231], micro-structured FBGs were functionalized by single-stranded DNA (ssDNA) aptamer to bio-recognize complementary base sequences and form a stable double-stranded region. Results showed high specificity to detect low target concentration in real-time. The main issues are related to difficulties in performing reproducible fabrication processes. Indeed, the washing process with a phosphate buffer saline solution followed by a re-hybridization led to a different number of active sites occupied by DNA molecules. Considering that the optical response is strongly dependent on the location of such binding sites on the fiber surface, also a different value of local sensitivity was achieved.

3) NEURODEGENERATIVE AND ENDOCRINE DISORDERS

DNA and enzyme-based biosensors have been developed for the diagnosis of neurodegenerative disorders (e.g., depression, Parkinson's disease, and dementia), often caused by the abnormal value of small molecules such as S-adenosyl-L-homocysteine (AdoHcy) and dopamine. For instance, in [230], a gold-coated SPR TFBG was functionalized with ssDNA aptamer anchored on the graphene layer. The sensor showed a linear response with a dopamine concentration increment with high resolution. A similar study was proposed in [238], where the enzyme named Lysine methyltransferase (Set7) was used to functionalize the surface of the gold film-coated SPR-TFBG fiber to detect AdoHcy. Results showed the capability of detecting surrounding refractive index changes from the transmitted spectrum, allowing low concentrations measurements.

Another field of application in medical diagnostics regards endocrine disorders starting from the detection of the blood glucose level. Several studies proposed glucose oxidase (GOD)-based TFBG biosensors. In [239], GOD was immobilized on a GO-coated TFBG via the cross-linker1-ethyl-3-(3-dimethylaminopropyl) carbodiimide (EDC) and N- hydroxyl succinimide (NHS). The glucose level was measured starting from the refractive index changes, which occurred during the

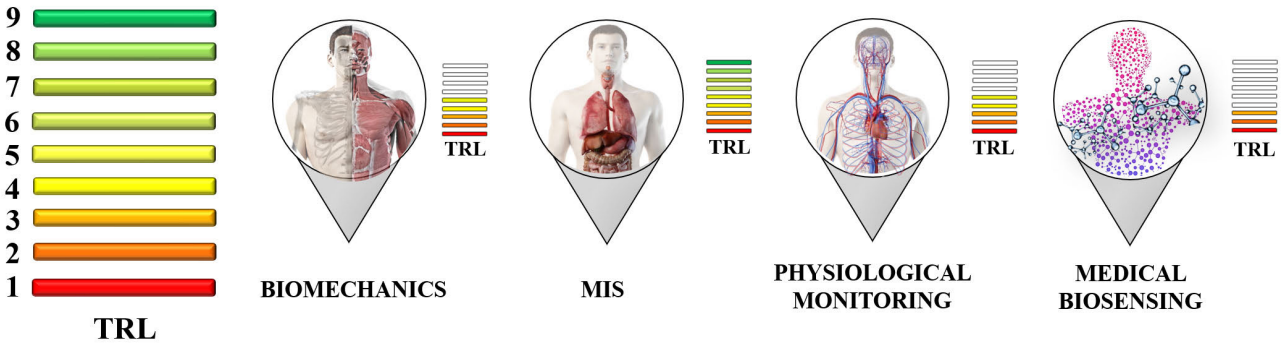

FIGURE 6. The TRL level of the FBG-based systems developed for biomechanics, MIS, physiological monitoring, and medical biosensing, respectively. The highest TRL value reached in each application is highlighted.

catalytic reaction of GOD. A sensitivity of 0.25 nm/mM was found in the range of low glucose concentrations between 0 nM and 8nM. Another TFBG sensor was used in [240], where the GOD enzyme was immobilized on a silanized optical fiber surface. The strong adhesion of GOD to the optical fiber due to the silanization process enabled the detection of low glucose concentration (0.013-0.02 mg/m).

IV. ADVANTAGES, CONSTRAINTS AND FUTURE CHALLENGES

In this article, a general overview of FBGs-based systems for medical applications has been brought out. The state-of-the-art of such solutions has been reviewed, ranging from applications in biomechanics and MIS, to physiological monitoring and medical biosensing. The ultimate aim of this work is to cover in-depth the working principle of sensing solutions based on FBGs and their applications in medicine. FBGs-based systems' advantages, main hurdles, and open challenges are discussed to point out their potentialities and the further steps necessary to translate this technology from research to clinical practice.

FBGs offer various advantages over conventional sensors, such as high sensitivity, high dynamic range, miniaturization, lightness, biocompatibility, chemical inertness, and multiplexing ability. Moreover, their electromagnetic immunity makes this optical solution feasible for application in harsh electromagnetic environments (e.g., inside the MR scanner). All these features enable the use of FBGs for various medical purposes. For instance, their small size, good metrological properties, and intrinsic biocompatibility are fundamental where high performance, intra-body insertion, and fabrics integration are required. These advantages are particularly attractive for applications in tissue biomechanics, manipulations, and thermal treatments, as well as in tool shaping and medical biosensing. The possibility to perform high resolved and distributed measurements enables the use of FBGs for monitoring joint kinematics, physiological parameters, and thermal treatment effects.

Recently, the Healthcare 4.0 revolution has placed demands of systems conformally attached to human bodies minimalizing discomfort and promoting a great deal of sensing functionalities. The achievement of such high expectations requires the development of skin-like flexible sensors more comfortable and performant than those currently proposed. For this reason, a considerable amount of research has been dedicated to the fabrication and characterization of FBG-based sensors encapsulated into soft matrices. Over the last years, several polymers have been investigated for grating encapsulations, and fastener solutions have been proposed (e.g., buttons, straps, tapes) improving the FBGs robustness, handless, flexibility, and body parts adhesion. As a result, a growing acceptance of FBGs in clinical applications has been achieved.

Although the successful implementation of FBGs-based technologies in clinical trials has been proved, there are still challenges to encounter. A limited amount of solutions are currently used in clinical practice [7]. For instance, some FBGs-based systems have been tested in clinical trials for biomechanics, and physiological monitoring [5], [241], and patented surgical instruments have been proposed for tactile and shape sensing [242]–[245].

To show the maturity of FBGs-based solutions described in Section III, the technology readiness level (TRL) is illustrated in Fig. 6. All the implemented systems achieved a TRL ranging from 3 to 9. The highest level is around 3 for biosensing, 5 for both biomechanics and physiological monitoring, and 9 for MIS as commercial solutions certified EN60601 are available [161] (see Fig. 6).

The clinical acceptance of FBGs-based systems has been dampened by the need of both an interrogation unit and a physical connection between the interrogator and the optical fiber embedding the FBGs.

Recently, steps forward have been done to contain the optical interrogator bulkiness and related costs. Indeed, commercial solutions with package dimensions smaller than 40 mm $\times$ 40 mm $\times$ 50 mm and costs lower than \$ 7000 are available. The open challenge is to improve the performance of the miniaturized interrogators since they show lower resolution, lower interrogation speed, narrower wavelength bandwidth, smaller number channels, than the bulky interrogators.

Another open challenge regards the development of even more realistic simulations for studying the matrix-fiber surface interaction. This knowledge may be useful to develop optimized flexible sensors according to the application of interest.

Moreover, in a future perspective, improvements in FBG inscription process, containment of FBG array dimensions, quality of multicore fiber technology, and temperature self-compensation will extend the market potential of FBG-based devices in medicine and healthcare.

The considerable amount of attention given to FBGs in scientific papers and the growing market interest regarding their applications in medicine (e.g., the increase of emerging and up-to-date sensing solutions for wearables, biosensing and shape sensing) underline the strong interest to fulfill the gap between research and clinical practice [8], [7]. Once the aforementioned challenges will be addressed and future trends realized, the next generation of medical devices will exploit the advantages of FBGs into portable solutions. The miniaturization of high-performant interrogation units and the development of optimized FBG-based sensing solutions as well as the incorporation of wireless data communication modulus and the implementation of direct control strategies will push the establishment of e-Health architectures based on fiber optics. Such innovation will encourage the extensive use of FBG-based technology in medicine and will contribute to make it an effective integral part of medical devices and healthcare system.

REFERENCES

[1] A. G. Leal-Junior, C. A. R. Diaz, L. M. Avellar, M. J. Pontes, C. Marques, and A. Frizera, "Polymer optical fiber sensors in healthcare applications: A comprehensive review," *Sensors*, vol. 19, no. 14, p. 3156, Jul. 2019.

[2] W. He, D. Goodkind, and P. Kowal, "International population reports: An aging world: 2015," U.S. Census Bureau, Suitland-Silver Hill, MD, USA, 2016, p. P95.

[3] D. Sharma, G. S. Aujla, and R. Bajaj, "Evolution from ancient medication to human-centered healthcare 4.0: A review on health care recommender systems," *Int. J. Commun. Syst.*, p. e4058, Sep. 2019. [Online]. Available: https://onlinelibrary.wiley.com/action/doSearch?AllField=Evolution+from+ancient+medication+to+human%E2%80%90centered+Healthcare+4.0%3A+A+review+on+health+care+recommender+systems&SeriesKey=10991131

[4] V. Mishra, N. Singh, U. Tiwari, and P. Kapur, "Fiber grating sensors in medicine: Current and emerging applications," *Sens. Actuators A, Phys.*, vol. 167, no. 2, pp. 279–290, Jun. 2011.

[5] E. Al-Fakih, N. A. A. Osman, and F. R. M. Adikan, "The use of fiber Bragg grating sensors in biomechanics and rehabilitation applications: The state-of-the-art and ongoing research topics," *Sensors*, vol. 12, no. 10, pp. 12890–12926, Sep. 2012.

[6] Y. J. Rao, "Optical in-fiber Bragg grating sensor systems for medical applications," *J. Biomed. Opt.*, vol. 3, no. 1, p. 38, Jan. 1998.

[7] R. Correia, S. James, S. W. Lee, S. P. Morgan, and S. Korposh, "Biomedical application of optical fibre sensors," *J. Opt.*, vol. 20, no. 7, p. 73003, 2018.

[8] M. D. Al-Amri, M. El-Gomati, and M. S. Zubairy, *Optics in Our Time*. Cham, Switzerland: Springer, 2016.

[9] A. Othonos, K. Kalli, and G. E. Kohnke, "Fiber Bragg gratings: Fundamentals and applications in telecommunications and sensing," *Phys. Today*, vol. 53, no. 5, pp. 61–62, May 2000.

[10] A. D. Kersey, M. A. Davis, H. J. Patrick, M. LeBlanc, K. P. Koo, C. G. Askins, M. A. Putnam, and E. J. Friebele, "Fiber grating sensors," *J. Lightw. Technol.*, vol. 15, no. 8, pp. 1442–1462, Aug. 1997.

[11] T. Erdogan, "Fiber grating spectra," *J. Lightw. Technol.*, vol. 15, no. 8, pp. 1277–1294, 1997.

[12] D. Tosi, "Review and analysis of peak tracking techniques for fiber Bragg grating sensors," *Sensors*, vol. 17, no. 10, p. 2368, Oct. 2017.

[13] D. Tosi, "Review of chirped fiber Bragg grating (CFBG) fiber-optic sensors and their applications," *Sensors*, vol. 18, no. 7, p. 2147, Jul. 2018.

[14] G. Palumbo, D. Tosi, A. Iadicicco, and S. Campopiano, "Analysis and design of chirped fiber Bragg grating for temperature sensing for possible biomedical applications," *IEEE Photon. J.*, vol. 10, no. 3, pp. 1–15, Jun. 2018.

[15] S. Korganbayev, Y. Orazayev, S. Sovetov, A. Bazyl, E. Schena, C. Massaroni, R. Gassino, A. Vallan, G. Perrone, P. Saccomandi, M. A. Caponero, G. Palumbo, S. Campopiano, A. Iadicicco, and D. Tosi, "Detection of thermal gradients through fiber-optic chirped fiber Bragg grating (CFBG): Medical thermal ablation scenario," *Opt. Fiber Technol.*, vol. 41, pp. 48–55, Mar. 2018.

[16] P. Bettini, E. Guerreschi, and G. Sala, "Development and experimental validation of a numerical tool for structural health and usage monitoring systems based on chirped grating sensors," *Sensors*, vol. 15, no. 1, pp. 1321–1341, Jan. 2015.

[17] J. Albert, L. Y. Shao, and C. Caucheteur, "Tilted fiber Bragg grating sensors," *Laser Photon. Rev.*, vol. 7, no. 1, pp. 83–108, Jan. 2013.

[18] T. Guo, F. Liu, B.-O. Guan, and J. Albert, "Tilted fiber grating mechanical and biochemical sensors," *Opt. Laser Technol.*, vol. 78, pp. 19–33, 2016.

[19] T. Guo, Á. González-Vila, M. Loyez, and C. Caucheteur, "Plasmonic optical fiber-grating immunosensing: A review," *Sensors*, vol. 17, no. 12, p. 2732, Nov. 2017.

[20] A. Bekmurzayeva, K. Dukenbayev, M. Shaimerdenova, I. Bekniyazov, T. Ayupova, M. Sypabekova, C. Molardi, and D. Tosi, "Etched fiber Bragg grating biosensor functionalized with aptamers for detection of thrombin," *Sensors*, vol. 18, no. 12, p. 4298, Dec. 2018.

[21] A. Iadicicco, A. Cusano, A. Cutolo, R. Bernini, and M. Giordano, "Thinned fiber Bragg gratings as high sensitivity refractive index sensor," *IEEE Photon. Technol. Lett.*, vol. 16, no. 4, pp. 1149–1151, Apr. 2004.

[22] D. Tosi, E. Schena, C. Molardi, and S. Korganbayev, "Fiber optic sensors for sub-centimeter spatially resolved measurements: Review and biomedical applications," *Opt. Fiber Technol.*, vol. 43, pp. 6–19, Jul. 2018.

[23] P. Saccomandi, C. M. Oddo, L. Zollo, D. Formica, R. A. Romeo, C. Massaroni, M. A. Caponero, N. Vitiello, E. Guglielmelli, S. Silvestri, and E. Schena, "Feedforward neural network for force coding of an MRI-compatible tactile sensor array based on fiber Bragg grating," *J. Sensors*, vol. 2015, pp. 1–9, Oct. 2015.

[24] L. Massari, E. Schena, C. Massaroni, P. Saccomandi, A. Menciassi, E. Sinibaldi, and C. M. Oddo, "A machine-learning-based approach to solve both contact location and force in soft material tactile sensors," *Soft Robot.*, vol. 7, no. 4, pp. 409–420, Aug. 2020.

[25] T.-W. Lu and C.-F. Chang, "Biomechanics of human movement and its clinical applications," *Kaohsiung J. Med. Sci.*, vol. 28, no. 2, pp. S13–S25, Feb. 2012.

[26] P. Roriz, A. Ramos, M. B. Marques, J. A. Simões, and O. Frazão, "A fiber optic buckle transducer for measurement of *in vitro* tendon strain," in *Proc. 24th Int. Conf. Opt. Fibre Sensors*, vol. 9634, 2015, p. 96342Q.

[27] L. Ren, G. Song, M. Conditt, P. C. Noble, and H. Li, "Fiber Bragg grating displacement sensor for movement measurement of tendons and ligaments," *Appl. Opt.*, vol. 46, no. 28, pp. 6867–6871, Oct. 2007.

[28] G. P. Behrmann, J. Hidler, and M. S. Mirotznik, "Fiber optic micro sensor for the measurement of tendon forces," *Biomed. Eng. Online*, vol. 11, no. 1, pp. 1–16, Oct. 2012.

[29] M. Vilimek, "Using a fiber Bragg grating sensor for tendon force measurements," *J. Biomech.*, vol. 41, p. S511, Jul. 2008.

[30] M. J. Paulsen, J. H. Bae, A. M. Imbrie-Moore, H. Wang, C. E. Hironaka, J. M. Farry, H. Lucian, A. D. Thakore, M. R. Cutkosky, and Y. J. Woo, "Development and *ex vivo* validation of novel force-sensing neochordae for measuring chordae tendineae tension in the mitral valve apparatus using optical fibers with embedded Bragg gratings," *J. Biomechanical Eng.*, vol. 142, no. 1, Jan. 2020.

[31] S. Iwanuma, R. Akagi, S. Hashizume, H. Kanehisa, T. Yanai, and Y. Kawakami, "Triceps surae muscle–tendon unit length changes as a function of ankle joint angles and contraction levels: The effect of foot arch deformation," *J. Biomech.*, vol. 44, no. 14, pp. 2579–2583, Sep. 2011.

[32] S. Iwanuma, R. Akagi, T. Kurihara, S. Ikegawa, H. Kanehisa, T. Fukunaga, and Y. Kawakami, "Longitudinal and transverse deformation of human achilles tendon induced by isometric plantar flexion at different intensities," *J. Appl. Physiol.*, vol. 110, no. 6, pp. 1615–1621, Jun. 2011.

[33] R. Akagi, S. Iwanuma, S. Hashizume, H. Kanehisa, T. Yanai, and Y. Kawakami, "*In vivo* measurements of moment arm lengths of three elbow flexors at rest and during isometric contractions," *J. Appl. Biomech.*, vol. 28, no. 1, pp. 63–69, Feb. 2012.

[34] T. Fresvig, P. Ludvigsen, H. Steen, and O. Reikerås, "Fibre optic Bragg grating sensors: An alternative method to strain gauges for measuring deformation in bone," *Med. Eng. Phys.*, vol. 30, no. 1, pp. 104–108, Jan. 2008.

[35] P. M. Talaia, A. Ramos, I. Abe, M. W. Schiller, P. Lopes, R. N. Nogueira, J. L. Pinto, R. Claramunt, and J. A. Simões, "Plated and intact femur strains in fracture fixation using fiber Bragg gratings and strain gauges," *Exp. Mech.*, vol. 47, no. 3, pp. 355–363, May 2007.

[36] A. Najafzadeh, T. Tran, B. K. Chen, J. Fu, D. S. Gunawardena, Z. Liu, and H.-Y. Tam, "Healing assessment of fractured femur by strain measurement using fibre Bragg grating sensors," in *Proc. Int. Conf. Sens. Instrum. IoT Era (ISSI)*, 2019, pp. 1–6.

[37] V. Mishra, N. Singh, D. V. Rai, U. Tiwari, G. C. Poddar, S. C. Jain, S. K. Mondal, and P. Kapur, "Fiber Bragg grating sensor for monitoring bone decalcification," *Orthopaedics Traumatol. Surg. Res.*, vol. 96, no. 6, pp. 646–651, Oct. 2010.

[38] S. Umesh, S. Padma, S. Asokan, and T. Srinivas, "Fiber Bragg grating based bite force measurement," *J. Biomechanics*, vol. 49, no. 13, pp. 2877–2881, Sep. 2016.

[39] A. Kalinowski, L. Zen Karam, V. Pegorini, A. B. Di Renzo, C. S. R. Pitta, R. Cardoso, T. S. Assmann, H. J. Kalinowski, and J. C. C. da Silva, "Optical fiber Bragg grating strain sensor for bone stress analysis in bovine during masticatory movements," *IEEE Sensors J.*, vol. 17, no. 8, pp. 2385–2392, Apr. 2017.

[40] G. Marchi, V. Baier, P. Alberton, P. Foehr, R. Burgkart, A. Aszodi, H. Clausen-Schaumann, and J. Roths, "Microindentation sensor system based on an optical fiber Bragg grating for the mechanical characterization of articular cartilage by stress-relaxation," *Sens. Actuators B, Chem.*, vol. 252, pp. 440–449, Nov. 2017.

[41] A. Aszodi, O. Canti, V. Baier, W. Micallef, B. Hartmann, P. Alberton, A. Aszodi, H. Clausen-Schaumann, and J. Roths, "Cartilage microindentation using cylindrical and spherical optical fiber indenters with integrated Bragg gratings as force sensors," *Proc. SPIE*, vol. 10496, Feb. 2018, p. 34.

[42] A. Javadzadeh Kalahrodi, G. Marchi, J. Möller, S. Nolte, and J. Roths, "2D stiffness mapping for localizing osteoarthritic degenerated cartilage by using a fast indentation system based on fiber Bragg gratings," in *Proc. 7th Eur. Workshop Opt. Fibre Sensors*, vol. 11199, Aug. 2019, p. 16.

[43] G. Marchi, P. Foehr, S. Consalvo, A. Javadzadeh-Kalarhodi, J. Lang, B. Hartmann, P. Alberton, A. Aszodi, R. Burgkart, and J. Roths, "Fiberoptic microindentation technique for early osteoarthritis diagnosis: An *in vitro* study on human cartilage," *Biomed. Microdevices*, vol. 21, no. 1, pp. 1–9, Mar. 2019.

[44] S. Umesh, S. Padma, T. Srinivas, and S. Asokan, "Fiber Bragg grating goniometer for joint angle measurement," *IEEE Sensors J.*, vol. 18, no. 1, pp. 216–222, Jan. 2018.

[45] S. Pant, S. Umesh, and S. Asokan, "Knee angle measurement device using fiber Bragg grating sensor," *IEEE Sensors J.*, vol. 18, no. 24, pp. 10034–10040, Dec. 2018.

[46] R. P. Rocha, A. F. Silva, J. P. Carmo, and J. H. Correia, "FBG in PVC foils for monitoring the knee joint movement during the rehabilitation process," in *Proc. Annu. Int. Conf. IEEE Eng. Med. Biol. Soc. (EMBS)*, Aug. 2011, pp. 458–461.

[47] Z. A. Abro, Y.-F. Zhang, C.-Y. Hong, R. A. Lakho, and N.-L. Chen, "Development of a smart garment for monitoring body postures based on FBG and flex sensing technologies," *Sens. Actuators A, Phys.*, vol. 272, pp. 153–160, Apr. 2018.

[48] Z. A. Abro, C. Hong, N. Chen, Y. Zhang, R. A. Lakho, and S. Yasin, "A fiber Bragg grating-based smart wearable belt for monitoring knee joint postures," *Textile Res. J.*, vol. 90, nos. 3–4, pp. 386–394, Feb. 2020.

[49] D. L. Presti, C. Massaroni, J. Di Tocco, E. Schena, A. Carnevale, U. G. Longo, J. D'Abbraccio, L. Massari, C. M. Oddo, and M. A. Caponero, "Single-plane neck movements and respiratory frequency monitoring: A smart system for computer workers," in *Proc. II Workshop Metrology Ind. 4.0 IoT (MetroInd4.0&IoT)*, Jun. 2019, pp. 167–170.

[50] D. Lo Presti, A. Carnevale, J. D'Abbraccio, L. Massari, C. Massaroni, R. Sabbadini, M. Zaltieri, J. Di Tocco, M. Bravi, S. Miccinilli, S. Sterzi, U. G. Longo, V. Denaro, M. A. Caponero, D. Formica, C. M. Oddo, and E. Schena, "A multi-parametric wearable system to monitor neck movements and respiratory frequency of computer workers," *Sensors*, vol. 20, no. 2, p. 536, Jan. 2020.

[51] H. Cheng-Yu, Z. A. Abro, Z. Yi-Fan, and R. A. Lakho, "An FBG-based smart wearable ring fabricated using FDM for monitoring body joint motion," *J. Ind. Textiles*, Aug. 2019, Art. no. 152808371987020. [Online]. Available: https://journals.sagepub.com/doi/full/10.1177/1528083719870204?casa_token=9eoVpVfaa5sAAAAA%3A0bzQ3PJDbRrY1JvJBDG80T3sBoM2c-99ZhAEOYliEjjQuVQTWLPaX4uuIblO8OU4yafroLd8CxVBb

[52] J. S. Kim, B. K. Kim, M. Jang, K. Kang, D. E. Kim, B.-K. Ju, and J. Kim, "Wearable hand module and real-time tracking algorithms for measuring finger joint angles of different hand sizes with high accuracy using FBG strain sensor," *Sensors*, vol. 20, no. 7, p. 1921, Mar. 2020.

[53] M. F. Domingues, A. Nepomuceno, C. Tavares, A. Radwan, N. Alberto, C. Marques, J. Rodriguez, P. Andre, and P. Antunes, "Energy-aware wearable E-health architecture using optical FBG sensors for knee kinematic monitoring," in *Proc. IEEE Global Commun. Conf. (GLOBECOM)*, Dec. 2018, pp. 1–6.

[54] M. F. Domingues, C. Tavares, V. Rosa, L. Pereira, N. Alberto, P. Andre, P. Antunes, and A. Radwan, "Wearable eHealth system for physical rehabilitation: Ankle plantar-dorsi-flexion monitoring," in *Proc. IEEE Global Commun. Conf. (GLOBECOM)*, Dec. 2019, pp. 1–6.

[55] P. W. Kong, C. C. Chan, M. L. Heng, Y. Liu, Y. Leow, and D. T. P. Fong, "Fiber Bragg grating sensors for clinical measurement of the first metatarsophalangeal joint quasi-stiffness," *IEEE Sensors J.*, vol. 20, no. 3, pp. 1322–1328, Feb. 2020.

[56] A. F. da Silva, A. F. Gonçalves, P. M. Mendes, and J. H. Correia, "FBG sensing glove for monitoring hand posture," *IEEE Sensors J.*, vol. 11, no. 10, pp. 2442–2448, Oct. 2011.

[57] M. Zaltieri, D. L. Presti, C. Massaroni, E. Schena, J. D'Abbraccio, L. Massari, C. M. Oddo, D. Formica, M. A. Caponero, M. Bravi, S. Miccinilli, and S. Sterzi, "Feasibility assessment of an FBG-based wearable system for monitoring back dorsal flexion-extension in video terminal workers," in *Proc. IEEE Int. Instrum. Meas. Technol. Conf. (I2MTC)*, May 2020, pp. 1–5.

[58] C. R. Dennison, P. M. Wild, D. R. Wilson, and M. K. Gilbart, "An in-fiber Bragg grating sensor for contact force and stress measurements in articular joints," *Meas. Sci. Technol.*, vol. 21, no. 11, Oct. 2010, Art. no. 115803.

[59] C. R. Dennison, P. M. Wild, P. W. G. Byrnes, A. Saari, E. Itshayek, D. C. Wilson, Q. A. Zhu, M. F. S. Dvorak, P. A. Cripton, and D. R. Wilson, "*Ex vivo* measurement of lumbar intervertebral disc pressure using fibre-Bragg gratings," *J. Biomechanics*, vol. 41, no. 1, pp. 221–225, Jan. 2008.

[60] S. Ambastha, S. Umesh, S. Dabir, and S. Asokan, "Comparison of force required for lumbar puncture with different gauges of spinal needle using fiber Bragg grating force device," *IEEE Sensors J.*, vol. 18, no. 19, pp. 8028–8033, Oct. 2018.

[61] S. Ambastha, S. Umesh, S. Dabir, and S. Asokan, "Spinal needle force monitoring during lumbar puncture using fiber Bragg grating force device," *J. Biomed. Opt.*, vol. 21, no. 11, Nov. 2016, Art. no. 117002.

[62] L. Mohanty and S. C. Tjin, "Pressure mapping at orthopaedic joint interfaces with fiber Bragg gratings," *Appl. Phys. Lett.*, vol. 88, no. 8, Feb. 2006, Art. no. 083901.

[63] L. Mohanty, S. C. Tjin, D. T. T. Lie, S. E. C. Panganiban, and P. K. H. Chow, "Fiber grating sensor for pressure mapping during total knee arthroplasty," *Sens. Actuators A, Phys.*, vol. 135, no. 2, pp. 323–328, Apr. 2007.

[64] L. Armitage, G. Rajan, L. Kark, A. Simmons, and B. G. Prusty, "Simultaneous measurement of normal and shear stress using fiber Bragg grating sensors in prosthetic applications," *IEEE Sensors J.*, vol. 19, no. 17, pp. 7383–7390, Sep. 2019.

[65] A. Completo, F. Fonseca, C. Relvas, A. Ramos, and J. A. Simóes, "Improved stability with intramedullary stem after anterior femoral notching in total knee arthroplasty," *Knee Surg., Sports Traumatol., Arthroscopy*, vol. 20, no. 3, pp. 487–494, Mar. 2012.

[66] M. P. Whelan, R. P. Kenny, C. Cavalli, A. B. Lennon, and P. J. Prendergast, "Application of optical fibre Bragg grating sensors to the study of PMMA curing," in *Proc. 12th Conf. Eur. Soc. Biomech. Roy. Acad. Med. Ireland*, 2000, p. 252.

[67] C. Frias, O. Frazão, S. Tavares, A. Vieira, A. T. Marques, and J. Simóes, "Mechanical characterization of bone cement using fiber Bragg grating sensors," *Mater. Des.*, vol. 30, no. 5, pp. 1841–1844, May 2009.

[68] A. Ramos, M. W. Schiller, I. Abe, P. A. Lopes, and J. A. Simóes, "Experimental measurement and numerical validation of bone cement mantle strains of an *in vitro* hip replacement using optical FBG sensors," *Experim. Mech.*, vol. 52, no. 9, pp. 1267–1274, Jan. 2012.

[69] A. Bimis and D. Karalekas, "Experimental evaluation of hardening strains in a bioceramic material using an embedded optical sensor," *Meccanica*, vol. 50, no. 2, pp. 541–547, Feb. 2015.

[70] A. Bimis, D. Karalekas, N. Bouropoulos, D. Mouzakis, and S. Zaoutsos, "Monitoring of hardening and hygroscopic induced strains in a calcium phosphate bone cement using FBG sensor," *J. Mech. Behav. Biomed. Mater.*, vol. 60, pp. 195–202, Jul. 2016.

[71] J. R. Galvão, C. R. Zamarreño, C. Martelli, J. C. C. da Silva, F. J. Arregui, and I. R. Matías, "Smart carbon fiber transtibial prosthesis based on embedded fiber Bragg gratings," *IEEE Sensors J.*, vol. 18, no. 4, pp. 1520–1527, Feb. 2018.

[72] J. R. Galvão, C. R. Zamarreño, C. Martelli, J. C. C. da Silva, F. J. Arregui, and I. R. Matías, "Strain mapping in carbon-fiber prosthesis using optical fiber sensors," *IEEE Sensors J.*, vol. 17, no. 1, pp. 3–4, Jan. 2017.

[73] J. Feng and Q. Jiang, "Slip and roughness detection of robotic fingertip based on FBG," *Sens. Actuators A, Phys.*, vol. 287, pp. 143–149, Mar. 2019.

[74] L. Massari, C. M. Oddo, E. Sinibaldi, R. Detry, J. Bowkett, and K. C. Carpenter, "Tactile sensing and control of robotic manipulator integrating fiber Bragg grating strain-sensor," *Frontiers Neurorobot.*, vol. 13, p. 8, Apr. 2019.

[75] C. M. Oddo, S. Raspopovic, F. Artoni, A. Mazzoni, G. Spigler, F. Petrini, F. Giambattistelli, F. Vecchio, F. Miraglia, L. Zollo, G. D. Pino, D. Camboni, M. C. Carrozza, E. Guglielmelli, P. M. Rossini, U. Faraguna, and S. Micera, "Intraneural stimulation elicits discrimination of textural features by artificial fingertip in intact and amputee humans," *Elife*, vol. 5, p. e09148, Mar. 2016.

[76] C. M. Oddo, G. Valle, D. Camboni, I. Strauss, M. Barbaro, G. Barabino, R. Puddu, C. Carboni, L. Bisoni, J. Carpaneto, F. Vecchio, F. M. Petrini, S. Romeni, T. Czimmermann, L. Massari, R. D. Iorio, F. Miraglia, G. Granata, D. Pani, T. Stieglitz, L. Raffo, P. M. Rossini, and S. Micera, "Morphological neural computation restores discrimination of naturalistic textures in trans-radial amputees," *Sci. Rep.*, vol. 10, no. 1, p. 527, Dec. 2020.

[77] G. T. Kanellos, G. Papaioannou, D. Tsiokos, C. Mitrogiannis, G. Nianios, and N. Pleros, "Two dimensional polymer-embedded quasi-distributed FBG pressure sensor for biomedical applications," *Opt. Express*, vol. 18, no. 1, p. 179, Jan. 2010.

[78] N. Pleros, G. T. Kanellos, and G. Papaioannou, "Optical fiber sensors in orthopedic biomechanics and rehabilitation," in *Proc. 9th Int. Conf. Inf. Technol. Appl. Biomed. (ITAB)*, Nov. 2009, pp. 1–4.

[79] G. T. Kanellos, D. Tsiokos, N. Pleros, G. Papaioannou, P. Childs, and S. Pissadakis, "Enhanced durability FBG-based sensor pads for biomedical applications as human-machine interface surfaces," in *Proc. Int. Workshop Biophoton. (BIOPHOTONICS)*, 2011, pp. 1–3.

[80] E. A. Al-Fakih, N. A. A. Osman, F. R. M. Adikan, A. Eshraghi, and P. Jahanshahi, "Development and validation of fiber Bragg grating sensing pad for interface pressure measurements within prosthetic sockets," *IEEE Sensors J.*, vol. 16, no. 4, pp. 965–974, Feb. 2016.

[81] E. A. Al-Fakih, N. A. A. Osman, A. Eshraghi, and F. R. M. Adikan, "The capability of fiber Bragg grating sensors to measure amputees' trans-tibial stump/socket interface pressures," *Sensors*, vol. 13, no. 8, pp. 10348–10357, Aug. 2013.

[82] C. Tavares, M. F. Domingues, T. Paixão, N. Alberto, H. Silva, and P. Antunes, "Wheelchair pressure ulcer prevention using FBG based sensing devices," *Sensors*, vol. 20, no. 1, p. 212, Dec. 2019.

[83] K. Chethana, A. S. G. Prasad, S. N. Omkar, B. Vadiraj, and S. Asokan, "Design and development of optical sensor based ground reaction force measurement platform for gait and geriatric studies," *Int. J. Mech. Aerosp. Ind. Mechatron. Manuf. Eng.*, vol. 10, no. 1, pp. 60–64, 2016.

[84] Y. F. Zhang, C. Y. Hong, R. Ahmed, and Z. Ahmed, "A fiber Bragg grating based sensing platform fabricated by fused deposition modeling process for plantar pressure measurement," *Meas. J. Int. Meas. Confed.*, vol. 112, pp. 74–79, Dec. 2017.

[85] J. Z. Hao, K. M. Tan, S. C. Tjin, C. Y. Liaw, P. R. Chaudhuri, X. Guo, and C. Lu, "Design of a foot-pressure monitoring transducer for diabetic patients based on FBG sensors," in *Proc. Conf. Lasers Electro-Opt. Soc. Annu. Meeting (LEOS)*, vol. 1, 2003, pp. 23–24.

[86] R. Suresh, S. Bhalla, J. Hao, and C. Singh, "Development of a high resolution plantar pressure monitoring pad based on fiber Bragg grating (FBG) sensors," *Technol. Health Care*, vol. 23, no. 6, pp. 785–794, Oct. 2015.

[87] T.-C. Liang, J.-J. Lin, and L.-Y. Guo, "Plantar pressure detection with fiber Bragg gratings sensing system," *Sensors*, vol. 16, no. 10, p. 1766, Oct. 2016.

[88] D. Vilarinho, A. Theodosiou, C. Leitão, A. G. Leal-Junior, M. De Fátima Domingues, K. Kalli, P. André, P. Antunes, and C. Marques, "POFBG-embedded cork insole for plantar pressure monitoring," *Sensors*, vol. 17, no. 12, p. 2924, Dec. 2017.

[89] C. Tavares, M. Domingues, A. Frizera-Neto, T. Leite, C. Leitão, N. Alberto, C. Marques, A. Radwan, E. Rocon, P. André, and P. Antunes, "Gait shear and plantar pressure monitoring: A non-invasive OFS based solution for e-Health architectures," *Sensors*, vol. 18, no. 5, p. 1334, Apr. 2018.

[90] Z. Hao, K. Cook, J. Canning, H.-T. Chen, and C. Martelli, "3-D printed smart orthotic insoles: Monitoring a Person's gait step by step," *IEEE Sensors Lett.*, vol. 4, no. 1, pp. 1–4, Jan. 2020.

[91] M. F. Domingues, C. Tavares, C. Leitão, A. Frizera-Neto, N. Alberto, C. Marques, A. Radwan, J. Rodriguez, O. Postolache, E. Rocon, P. André, and P. Antunes, "Insole optical fiber Bragg grating sensors network for dynamic vertical force monitoring," *J. Biomed. Opt.*, vol. 22, no. 9, Feb. 2017, Art. no. 091507.

[92] M. F. Domingues, N. Alberto, C. S. J. Leitao, C. Tavares, E. Rocon de Lima, A. Radwan, V. Sucasas, J. Rodriguez, P. S. B. Andre, and P. F. C. Antunes, "Insole optical fiber sensor architecture for remote gait Analysis—An e-Health solution," *IEEE Internet Things J.*, vol. 6, no. 1, pp. 207–214, Feb. 2019.

[93] J. C. C. Silva, L. Carvalho, R. N. Nogueira, J. A. Simoes, J. L. Pinto, and H. J. Kalinowski, "FBG applied in dynamic analysis of an implanted cadaveric mandible," in *Proc. 2nd Eur. Workshop Opt. Fibre Sensors*, vol. 5502, 2004, p. 226.

[94] L. Carvalho, J. C. C. Silva, R. N. Nogueira, J. L. Pinto, H. J. Kalinowski, and J. A. Simúes, "Application of Bragg grating sensors in dental biomechanics," *J. Strain Anal. Eng. Des.*, vol. 41, no. 6, pp. 411–416, Aug. 2006.

[95] J. C. C. Silva, A. Ramos, L. Carvalho, R. N. Nogueira, A. Ballu, M. Mesnard, J. L. Pinto, H. J. Kalinowski, and J. A. Simoes, "Fibre Bragg grating sensing and finite element analysis of the biomechanics of the mandible," in *Proc. 17th Int. Conf. Opt. Fibre Sensors*, vol. 5855, May 2005, p. 102.

[96] M. W. Schiller, I. Abe, P. Carvalho, P. Lopes, L. Carvalho, R. N. Nogueira, J. L. Pinto, and J. A. Simões, "On the use of FBG sensors to assess the performance of a dental implant system," in *Proc. Opt. InfoBase Conf. Papers*, 2006, p. ThE77, Paper ThE77.

[97] H. Kalinowski, J. Simoes, J. Pinto, L. Carvalho, R. Nogueira, J. Silva, and M. Milczewski, "Probing dental biomechanics with fibre Bragg grating sensors," in *Proc. 7th Int. Conf.*, Dec. 2004.

[98] M. S. Milczewski, J. C. C. da Silva, I. Abe, L. Carvalho, C. Fernandes, H. J. Kalinowski, and R. N. Nogueira, "FBG application in the determination of setting expansion of dental materials," in *Proc. 17th Int. Conf. Opt. Fibre Sensors*, vol. 5855, May 2005, p. 387.

[99] H. Ottevaere, M. Tabak, A. F. Fernandez, F. Berghmans, and H. Thienpont, "Optical fiber sensors and their application in monitoring stress build-up in dental resin cements," *Proc. SPIE*, vol. 5952, Sep. 2005, Art. no. 59520P.

[100] S. C. Tjin, Y. K. Tan, M. Yow, Y.-Z. Lam, and J. Hao, "Recording compliance of dental splint use in obstructive sleep apnoea patients by force and temperature modelling," *Med. Biol. Eng. Comput.*, vol. 39, no. 2, pp. 182–184, Mar. 2001.

[101] M. S. Milczeswki, J. C. C. Silva, I. Abe, J. A. Simóes, A. S. Paterno, and H. J. Kalinowski, "Measuring orthodontic forces with HiBi FBG sensors," in *Proc. Opt. InfoBase Conf. Papers*, 2006, p. TuE65, Paper TuE65.
[102] M. S. Milczewski, H. J. Kalinowski, J. C. C. da Silva, I. Abe, J. A. Simóes, and A. Saga, "Stress monitoring in a maxilla model and dentition," in *Proc. 21st Int. Conf. Opt. Fiber Sensors*, vol. 7753, May 2011, p. 77534.
[103] L. Carvalho, P. Roriz, O. Frazão, and M. B. Marques, "Evaluation of the performance of orthodontic devices using FBG sensors," *J. Phys. Conf. Ser.*, vol. 605, no. 1, p. 12017, 2015.
[104] V. Vitiello, K.-W. Kwok, and G.-Z. Yang, "Introduction to robot-assisted minimally invasive surgery (MIS)," in *Medical Robotics*. Amsterdam, The Netherlands: Elsevier, 2012, p. 1-P1.
[105] A. Abushagur, N. Arsad, M. Reaz, and A. Bakar, "Advances in bio-tactile sensors for minimally invasive surgery using the fibre Bragg grating force sensor technique: A survey," *Sensors*, vol. 14, no. 4, pp. 6633–6665, Apr. 2014.
[106] C. Shi, X. Luo, P. Qi, T. Li, S. Song, Z. Najdovski, T. Fukuda, and H. Ren, "Shape sensing techniques for continuum robots in minimally invasive surgery: A survey," *IEEE Trans. Biomed. Eng.*, vol. 64, no. 8, pp. 1665–1678, Aug. 2017.
[107] J. Konstantinova, A. Jiang, K. Althoefer, P. Dasgupta, and T. Nanayakkara, "Implementation of tactile sensing for palpation in robot-assisted minimally invasive surgery: A review," *IEEE Sensors J.*, vol. 14, no. 8, pp. 2490–2501, Aug. 2014.
[108] Z. Wang, S. Wang, and S. Zuo, "A hand-held device with 3-DOF haptic feedback mechanism for microsurgery," *Int. J. Med. Robot. Comput. Assist. Surg.*, vol. 15, no. 5, p. e2025, Oct. 2019.
[109] Z. Sun, M. Balicki, J. Kang, J. Handa, R. Taylor, and I. Iordachita, "Development and preliminary data of novel integrated optical micro-force sensing tools for retinal microsurgery," in *Proc. IEEE Int. Conf. Robot. Autom.*, May 2009, pp. 1897–1902.
[110] I. Iordachita, Z. Sun, M. Balicki, J. U. Kang, S. J. Phee, J. Handa, P. Gehlbach, and R. Taylor, "A sub-millimetric, 0.25 mN resolution fully integrated fiber-optic force-sensing tool for retinal microsurgery," *Int. J. Comput. Assist. Radiol. Surg.*, vol. 4, no. 4, pp. 383–390, Apr. 2009.
[111] X. He, J. Handa, P. Gehlbach, R. Taylor, and I. Iordachita, "A sub-millimetric 3-DOF force sensing instrument with integrated fiber Bragg grating for retinal microsurgery," *IEEE Trans. Biomed. Eng.*, vol. 61, no. 2, pp. 522–534, Feb. 2014.
[112] S. Sunshine, M. Balicki, X. He, K. Olds, J. U. Kang, P. Gehlbach, R. Taylor, I. Iordachita, and J. T. Handa, "A force-sensing microsurgical instrument that detects forces below human tactile sensation," *Retina*, vol. 33, no. 1, pp. 200–206, Jan. 2013.
[113] B. Gonenc, M. A. Balicki, J. Handa, P. Gehlbach, C. N. Riviere, R. H. Taylor, and I. Iordachita, "Preliminary evaluation of a micro-force sensing handheld robot for vitreoretinal surgery," in *Proc. IEEE/RSJ Int. Conf. Intell. Robots Syst.*, Oct. 2012, pp. 4125–4130.
[114] A. Gijbels, E. B. Vander Poorten, P. Stalmans, and D. Reynaerts, "Development and experimental validation of a force sensing needle for robotically assisted retinal vein cannulations," in *Proc. IEEE Int. Conf. Robot. Autom.*, May 2015, pp. 2270–2276.
[115] A. Gijbels, K. Willekens, L. Esteveny, P. Stalmans, D. Reynaerts, and E. B. Vander Poorten, "Towards a clinically applicable robotic assistance system for retinal vein cannulation," in *Proc. 6th IEEE Int. Conf. Biomed. Robot. Biomechatron.*, Jun. 2016, pp. 284–291.
[116] B. Gonenc, R. H. Taylor, I. Iordachita, P. Gehlbach, and J. Handa, "Force-sensing microneedle for assisted retinal vein cannulation," in *Proc. IEEE Sensors*, Nov. 2014, pp. 698–701.
[117] B. Gonenc, N. Tran, C. N. Riviere, P. Gehlbach, R. H. Taylor, and I. Iordachita, "Force-based puncture detection and active position holding for assisted retinal vein cannulation," in *Proc. IEEE Int. Conf. Multisensor Fusion Integr. Intell. Syst.*, Sep. 2015, pp. 322–327.
[118] B. Gonenc, A. Chamani, J. Handa, P. Gehlbach, R. H. Taylor, and I. Iordachita, "3-DOF force-sensing motorized micro-forceps for robot-assisted vitreoretinal surgery," *IEEE Sensors J.*, vol. 17, no. 11, pp. 3526–3541, Jun. 2017.
[119] B. Gonenc, N. Patel, and I. Iordachita, "Evaluation of a force-sensing handheld robot for assisted retinal vein Cannulation*," in *Proc. Annu. Int. Conf. IEEE Eng. Med. Biol. Soc. (EMBC)*, Jul. 2018, pp. 1–5.
[120] X. He, M. A. Balicki, J. U. Kang, P. L. Gehlbach, J. T. Handa, R. H. Taylor, and I. I. Iordachita, "Force sensing micro-forceps with integrated fiber Bragg grating for vitreoretinal surgery," *Proc. SPIE*, vol. 8218, Jan. 2012, Art. no. 82180W.
[121] I. Kuru, B. Gonenc, M. Balicki, J. Handa, P. Gehlbach, R. H. Taylor, and I. Iordachita, "Force sensing micro-forceps for robot assisted retinal surgery," in *Proc. Annu. Int. Conf. IEEE Eng. Med. Biol. Soc.*, Aug. 2012, pp. 1401–1404.
[122] X. He, M. Balicki, P. Gehlbach, J. Handa, R. Taylor, and I. Iordachita, "A multi-function force sensing instrument for variable admittance robot control in retinal microsurgery," in *Proc. IEEE Int. Conf. Robot. Autom.*, May 2014, pp. 1411–1418.
[123] A. Ebrahimi, N. Patel, C. He, P. Gehlbach, M. Kobilarov, and I. Iordachita, "Adaptive control of sclera force and insertion depth for safe robot-assisted retinal surgery," in *Proc. Int. Conf. Robot. Autom.*, May 2019, pp. 9073–9079.
[124] C. He, N. Patel, A. Ebrahimi, M. Kobilarov, and I. Iordachita, "Preliminary study of an RNN-based active interventional robotic system (AIRS) in retinal microsurgery," *Int. J. Comput. Assist. Radiol. Surg.*, vol. 14, no. 6, pp. 945–954, Mar. 2019.
[125] C. He, N. Patel, M. Shahbazi, Y. Yang, P. Gehlbach, M. Kobilarov, and I. Iordachita, "Toward safe retinal microsurgery: Development and evaluation of an RNN-based active interventional control framework," *IEEE Trans. Biomed. Eng.*, vol. 67, no. 4, pp. 966–977, Apr. 2020.
[126] C. Kim and C.-H. Lee, "Development of a 6-DoF FBG force–moment sensor for a haptic interface with minimally invasive robotic surgery," *J. Mech. Sci. Technol.*, vol. 30, no. 8, pp. 3705–3712, Aug. 2016.
[127] C. Lv, S. Wang, and C. Shi, "A high-precision and miniature fiber Bragg grating-based force sensor for tissue palpation during minimally invasive surgery," *Ann. Biomed. Eng.*, vol. 48, no. 2, pp. 669–681, Feb. 2020.
[128] R. Xue, B. Ren, J. Huang, Z. Yan, and Z. Du, "Design and evaluation of FBG-based tension sensor in laparoscope surgical robots," *Sensors*, vol. 18, no. 7, p. 2067, Jun. 2018.
[129] P. S. Zarrin, A. Escoto, R. Xu, R. V. Patel, M. D. Naish, and A. L. Trejos, "Development of a 2-DOF sensorized surgical grasper for grasping and axial force measurements," *IEEE Sensors J.*, vol. 18, no. 7, pp. 2816–2826, Apr. 2018.
[130] P. S. Zarrin, A. Escoto, R. Xu, R. V. Patel, M. D. Naish, and A. L. Trejos, "Development of an optical fiber-based sensor for grasping and axial force sensing," in *Proc. IEEE Int. Conf. Robot. Autom.*, May 2017, pp. 939–944.
[131] K. S. Shahzada, A. Yurkewich, R. Xu, and R. V. Patel, "Sensorization of a surgical robotic instrument for force sensing," *Proc. SPIE*, vol. 9702, Mar. 2016, Art. no. 97020U.
[132] Y. Guo, J. Kong, H. Liu, H. Xiong, G. Li, and L. Qin, "A three-axis force fingertip sensor based on fiber Bragg grating," *Sens. Actuators A, Phys.*, vol. 249, pp. 141–148, Oct. 2016.
[133] C. Shi, M. Li, C. Lv, J. Li, and S. Wang, "A high-sensitivity fiber Bragg grating-based distal force sensor for laparoscopic surgery," *IEEE Sensors J.*, vol. 20, no. 5, pp. 2467–2475, Mar. 2020.
[134] C. Huang, R. X. Huang, and Z. J. Qiu, "Natural orifce transluminal endoscopic surgery: New minimally invasive surgery come of age," *World J. Gastroenterol.*, vol. 17, no. 39, pp. 4382–4388, Oct. 2011.
[135] W. Lai, L. Cao, R. X. Tan, Y. C. Tan, X. Li, P. T. Phan, A. M. H. Tiong, S. C. Tjin, and S. J. Phee, "An integrated sensor-model approach for haptic feedback of flexible endoscopic robots," *Ann. Biomed. Eng.*, vol. 48, no. 1, pp. 342–356, Jan. 2020.
[136] W. Lai, L. Cao, R. X. Tan, P. T. Phan, J. Hao, S. C. Tjin, and S. J. Phee, "Force sensing with 1 mm fiber Bragg gratings for flexible endoscopic surgical robots," *IEEE/ASME Trans. Mechatronics*, vol. 25, no. 1, pp. 371–382, Feb. 2020.
[137] W. Lai, L. Cao, Z. Xu, P. T. Phan, P. Shum, and S. J. Phee, "Distal end force sensing with optical fiber Bragg gratings for tendon-sheath mechanisms in flexible endoscopic robots," in *Proc. IEEE Int. Conf. Robot. Autom.*, May 2018, pp. 5349–5355.
[138] J. W. Arkwright, N. G. Blenman, I. D. Underhill, S. A. Maunder, M. M. Szczesniak, P. G. Dinning, and I. J. Cook, "*In-vivo* demonstration of a high resolution optical fiber manometry catheter for diagnosis of gastrointestinal motility disorders," *Opt. Express*, vol. 17, no. 6, p. 4500, Mar. 2009.
[139] F. Bianchi, E. Trallori, D. Camboni, C. M. Oddo, A. Menciassi, G. Ciuti, and P. Dario, "Endoscopic tactile instrument for remote tissue palpation in colonoscopic procedures," in *Proc. IEEE Int. Conf. Cyborg Bionic Syst.*, Oct. 2017, pp. 248–252.
[140] J. H. Bae, C. J. Ploch, M. A. Lin, B. L. Daniel, and M. R. Cutkosky, "Display of needle tip contact forces for steering guidance," in *Proc. IEEE Haptics Symp. (HAPTICS)*, Apr. 2016, pp. 332–337.

[141] B. Carotenuto, A. Micco, A. Ricciardi, E. Amorizzo, M. Mercieri, A. Cutolo, and A. Cusano, "Optical guidance systems for epidural space identification," *IEEE J. Sel. Topics Quantum Electron.*, vol. 23, no. 2, pp. 371–379, Mar. 2017.

[142] S. Elayaperumal, J. H. Bae, B. L. Daniel, and M. R. Cutkosky, "Detection of membrane puncture with haptic feedback using a tip-force sensing needle," in *Proc. IEEE/RSJ Int. Conf. Intell. Robots Syst.*, Sep. 2014, pp. 3975–3981.

[143] M. Ahmed, C. L. Brace, F. T. Lee, and S. N. Goldberg, "Principles of and advances in percutaneous ablation," *Radiology*, vol. 258, no. 2, pp. 351–369, Feb. 2011.

[144] E. Schena, D. Tosi, P. Saccomandi, E. Lewis, and T. Kim, "Fiber optic sensors for temperature monitoring during thermal treatments: An overview," *Sensors*, vol. 16, no. 7, p. 1144, Jul. 2016.

[145] P. Saccomandi, E. Schena, and S. Silvestri, "Techniques for temperature monitoring during laser-induced thermotherapy: An overview," *Int. J. Hyperthermia*, vol. 29, no. 7, pp. 609–619, Nov. 2013.

[146] Y. J. Rao, D. J. Webb, D. A. Jackson, L. Zhang, and I. Bennion, "In-fiber bragg-grating temperature sensor system for medical applications," *J. Lightw. Technol.*, vol. 15, no. 5, pp. 779–784, May 1997.

[147] E. Samset, T. Mala, B. Edwin, I. Gladhaug, O. Søreide, and E. Fosse, "Validation of estimated 3D temperature maps during hepatic cryo surgery," *Magn. Reson. Imag.*, vol. 19, no. 5, pp. 715–721, Jun. 2001.

[148] N. T. Pham, S. L. Lee, S. Park, Y. W. Lee, and H. W. Kang, "Real-time temperature monitoring with fiber Bragg grating sensor during diffuser-assisted laser-induced interstitial thermotherapy," *J. Biomed. Opt.*, vol. 22, no. 4, Apr. 2017, Art. no. 045008.

[149] D. Polito, M. Arturo Caponero, A. Polimadei, P. Saccomandi, C. Massaroni, S. Silvestri, and E. Schena, "A needlelike probe for temperature monitoring during laser ablation based on fiber Bragg grating: Manufacturing and characterization," *J. Med. Devices*, vol. 9, no. 4, Dec. 2015.

[150] F. M. Di Matte, P. Saccomandi, M. Martino, M. Pandolfi, M. Pizzicannella, V. Balassone, E. Schena, C. M. Pacella, S. Silvestri, and G. Costamagna, "Feasibility of EUS-guided Nd:YAG laser ablation of unresectable pancreatic adenocarcinoma," *Gastrointest. Endosc.*, vol. 88, no. 1, pp. 168–174.e1, Jul. 2018.

[151] C. Cavaiola, P. Saccomandi, C. Massaroni, D. Tosi, F. Giurazza, G. Frauenfelder, B. Beomonte Zobel, F. M. Di Matteo, M. A. Caponero, A. Polimadei, and E. Schena, "Error of a temperature probe for cancer ablation monitoring caused by respiratory movements: *Ex vivo* and *in vivo* analysis," *IEEE Sensors J.*, vol. 16, no. 15, pp. 5934–5941, Aug. 2016.

[152] S. Ambastha, S. Pant, S. Umesh, V. Vazhayil, and S. Asokan, "Feasibility study on thermography of embedded tumor using fiber Bragg grating thermal sensor," *IEEE Sensors J.*, vol. 20, no. 5, pp. 2452–2459, Mar. 2020.

[153] H. H. Abd Raziff, D. Tan, K.-S. Lim, C. H. Yeong, Y. H. Wong, B. J. J. Abdullah, N. Sulaiman, and H. Ahmad, "A temperature-controlled laser hot needle with grating sensor for liver tissue tract ablation," *IEEE Trans. Instrum. Meas.*, vol. 69, no. 9, pp. 7119–7124, Sep. 2020.

[154] E. De Vita, M. Zaltieri, F. De Tommasi, C. Massaroni, E. Faiella, B. B. Zobel, A. Iadicicco, E. Schena, R. F. Grasso, and S. Campopiano, "Multipoint temperature monitoring of microwave thermal ablation in bones through fiber Bragg grating sensor arrays," *Sensors*, vol. 20, no. 11, p. 3200, Jun. 2020.

[155] S. Korganbayev, S. Asadi, A. Wolf, A. Dostovalov, M. Zalteri, E. Schena, H. Azhari, I. S. Weitz, and P. Saccomandi, "Highly dense FBG arrays for millimeter-scale thermal monitoring during nanocomposite-enhanced laser ablation," *Proc. SPIE*, vol. 11354, Apr. 2020, p. 19.

[156] E. Schena and L. Majocchi, "Assessment of temperature measurement error and its correction during nd:YAG laser ablation in porcine pancreas," *Int. J. Hyperthermia*, vol. 30, no. 5, pp. 328–334, Aug. 2014.

[157] F. Manns, P. J. Milne, X. Gonzalez-Cirre, D. B. Denham, J.-M. Parel, and D. S. Robinson, "*In situ* temperature measurements with thermocouple probes during laser interstitial thermotherapy (LITT): Quantification and correction of a measurement artifact," *Lasers Surgery Med.*, vol. 23, no. 2, pp. 94–103, 1998.

[158] A. D. Reid, M. R. Gertner, and M. D. Sherar, "Temperature measurement artefacts of thermocouples and fluoroptic probes during laser irradiation at 810 nm," *Phys. Med. Biol.*, vol. 46, no. 6, pp. N149–N157, Jun. 2001.

[159] G. Allegretti, P. Saccomandi, F. Giurazza, M. A. Caponero, G. Frauenfelder, F. M. Di Matteo, B. B. Zobel, S. Silvestri, and E. Schena, "Magnetic resonance-based thermometry during laser ablation on *ex-vivo* swine pancreas and liver," *Med. Eng. Phys.*, vol. 37, no. 7, pp. 631–641, Jul. 2015.

[160] E. Schena, P. Saccomandi, F. Giurazza, M. A. Caponero, L. Mortato, F. M. D. Matteo, F. Panzera, R. D. Vescovo, B. B. Zobel, and S. Silvestri, "Experimental assessment of CT-based thermometry during laser ablation of porcine pancreas," *Phys. Med. Biol.*, vol. 58, no. 16, p. 5705, 2013.

[161] *Shape Sensing—FBGS*. Accessed: Jun. 27, 2020. [Online]. Available: https://fbgs.com/solutions/shape-sensing/

[162] M. Abayazid, M. Kemp, and S. Misra, "3D flexible needle steering in soft-tissue phantoms using fiber Bragg grating sensors," in *Proc. IEEE Int. Conf. Robot. Autom.*, May 2013, pp. 5843–5849.

[163] R. J. Roesthuis, M. Kemp, J. J. van den Dobbelsteen, and S. Misra, "Three-dimensional needle shape reconstruction using an array of fiber Bragg grating sensors," *IEEE/ASME Trans. Mechatronics*, vol. 19, no. 4, pp. 1115–1126, Aug. 2014.

[164] Z. Lunwei, Q. Jinwu, S. Linyong, and Z. Yanan, "FBG sensor devices for spatial shape detection of intelligent colonoscope," in *Proc. IEEE Int. Conf. Robot. Autom.*, May 2004, pp. 835–840.

[165] X. Yi, J. Qian, Y. Zhang, Z. Zhang, and L. Shen, "3-D shape display of intelligent colonoscope based on FBG sensor array and binocular vision," in *Proc. IEEE/ICME Int. Conf. Complex Med. Eng.*, May 2007, pp. 14–19.

[166] I. Floris, P. A. Calderón, S. Sales, and J. M. Adam, "Effects of core position uncertainty on optical shape sensor accuracy," *Measurement*, vol. 139, pp. 21–33, Jun. 2019.

[167] F. Khan, A. Denasi, D. Barrera, J. Madrigal, S. Sales, and S. Misra, "Multi-core optical fibers with Bragg gratings as shape sensor for flexible medical instruments," *IEEE Sensors J.*, vol. 19, no. 14, pp. 5878–5884, Jul. 2019.

[168] R. Xu, A. Yurkewich, and R. V. Patel, "Shape sensing for torsionally compliant concentric-tube robots," *Proc. SPIE*, vol. 9702, Mar. 2016, Art. no. 97020V.

[169] N. J. van de Berg, J. Dankelman, and J. J. van den Dobbelsteen, "Design of an actively controlled steerable needle with tendon actuation and FBG-based shape sensing," *Med. Eng. Phys.*, vol. 37, no. 6, pp. 617–622, Jun. 2015.

[170] S. Jäckle, T. Eixmann, H. Schulz-Hildebrandt, G. Hüttmann, and T. Pätz, "Fiber optical shape sensing of flexible instruments for endovascular navigation," *Int. J. Comput. Assist. Radiol. Surg.*, vol. 14, no. 12, pp. 2137–2145, Dec. 2019.

[171] W. Q. Mok, W. Wang, and S. Y. Liaw, "Vital signs monitoring to detect patient deterioration: An integrative literature review," *Int. J. Nursing Pract.*, vol. 21, pp. 91–98, May 2015.

[172] C. Massaroni, M. Zaltieri, D. Lo Presti, D. Tosi, and E. Schena, "Fiber Bragg grating sensors for cardiorespiratory monitoring: A review," *IEEE Sensors J.*, early access, Apr. 1, 2020, doi: 10.1109/JSEN.2020.2988692.

[173] L. Dziuda, F. W. Skibniewski, M. Krej, and J. Lewandowski, "Monitoring respiration and cardiac activity using fiber Bragg grating-based sensor," *IEEE Trans. Biomed. Eng.*, vol. 59, no. 7, pp. 1934–1942, Jul. 2012.

[174] J. Hao, M. Jayachandran, P. L. Kng, S. F. Foo, P. W. Aung Aung, and Z. Cai, "FBG-based smart bed system for healthcare applications," *Frontiers Optoelectron. China*, vol. 3, no. 1, pp. 78–83, Jan. 2010.

[175] S. Iacoponi, C. Massaroni, D. Lo Presti, P. Saccomandi, M. A. Caponero, R. D'Amato, and E. Schena, "Polymer-coated fiber optic probe for the monitoring of breathing pattern and respiratory rate," in *Proc. Annu. Int. Conf. IEEE Eng. Med. Biol. Soc. (EMBC)*, Jul. 2018, pp. 1616–1619.

[176] D. Lo Presti, C. Romano, C. Massaroni, J. D'Abbraccio, L. Massari, M. A. Caponero, C. M. Oddo, D. Formica, and E. Schena, "Cardio-respiratory monitoring in archery using a smart textile based on flexible fiber Bragg grating sensors," *Sensors*, vol. 19, no. 16, p. 3581, Aug. 2019.

[177] M. Ciocchetti, C. Massaroni, P. Saccomandi, M. Caponero, A. Polimadei, D. Formica, and E. Schena, "Smart textile based on fiber Bragg grating sensors for respiratory monitoring: Design and preliminary trials," *Biosensors*, vol. 5, no. 3, pp. 602–615, Sep. 2015.

[178] C. Massaroni, M. Ciocchetti, G. Di Tomaso, P. Saccomandi, M. A. Caponero, A. Polimadei, D. Formica, and E. Schena, "Design and preliminary assessment of a smart textile for respiratory monitoring based on an array of fiber Bragg gratings," in *Proc. 38th Annu. Int. Conf. IEEE Eng. Med. Biol. Soc. (EMBC)*, Aug. 2016, pp. 6054–6057.

[179] G. Wehrle, P. Nohama, H. J. Kalinowski, P. I. Torres, and L. C. G. Valente, "A fibre optic Bragg grating strain sensor for monitoring ventilatory movements," *Meas. Sci. Technol.*, vol. 12, no. 7, pp. 805–809, Jul. 2001.

[180] A. Grillet, D. Kinet, J. Witt, M. Schukar, K. Krebber, F. Pirotte, and A. Depre, "Optical fiber sensors embedded into medical textiles for healthcare monitoring," *IEEE Sensors J.*, vol. 8, no. 7, pp. 1215–1222, Jul. 2008.

[181] J. De Jonckheere, F. Narbonneau, M. Jeanne, D. Kinet, J. Witt, K. Krebber, B. Paquet, A. Depre, and R. Logier, "OFSETH: Smart medical textile for continuous monitoring of respiratory motions under magnetic resonance imaging," in *Proc. Annu. Int. Conf. IEEE Eng. Med. Biol. Soc.*, Sep. 2009, pp. 1473–1476.

[182] J. Witt, F. Narbonneau, M. Schukar, K. Krebber, J. De Jonckheere, M. Jeanne, D. Kinet, B. Paquet, A. Depre, L. T. D'Angelo, T. Thiel, and R. Logier, "Medical textiles with embedded fiber optic sensors for monitoring of respiratory movement," *IEEE Sensors J.*, vol. 12, no. 1, pp. 246–254, Jan. 2012.

[183] D. L. Presti, C. Massaroni, D. Formica, P. Saccomandi, F. Giurazza, M. A. Caponero, and E. Schena, "Smart textile based on 12 fiber Bragg gratings array for vital signs monitoring," *IEEE Sensors J.*, vol. 17, no. 18, pp. 6037–6043, Sep. 2017.

[184] D. L. Presti, C. Massaroni, P. S. E. Schena, D. Formica, M. A. Caponero, and G. D. Tomaso, "Smart textile based on FBG sensors for breath-by-breath respiratory monitoring: Tests on women," in *Proc. IEEE Int. Symp. Med. Meas. Appl. (MeMeA)*, Jun. 2018, pp. 1–6.

[185] A. F. Silva, J. P. Carmo, P. M. Mendes, and J. H. Correia, "Simultaneous cardiac and respiratory frequency measurement based on a single fiber Bragg grating sensor," *Meas. Sci. Technol.*, vol. 22, no. 7, Jul. 2011, Art. no. 075801.

[186] J. Nedoma, M. Fajkus, M. Novak, N. Strbikova, V. Vasinek, H. Nazeran, J. Vanus, F. Perecar, and R. Martinek, "Validation of a novel fiber-optic sensor system for monitoring cardiorespiratory activities during MRI examinations," *Adv. Electr. Electron. Eng.*, vol. 15, no. 3, pp. 536–543, Oct. 2017.

[187] D. Lo Presti, C. Massaroni, J. D'Abbraccio, L. Massari, M. Caponero, U. G. Longo, D. Formica, C. M. Oddo, and E. Schena, "Wearable system based on flexible FBG for respiratory and cardiac monitoring," *IEEE Sensors J.*, vol. 19, no. 17, pp. 7391–7398, Sep. 2019.

[188] Ł. Dziuda, F. W. Skibniewski, M. Krej, and P. M. Baran, "Fiber Bragg grating-based sensor for monitoring respiration and heart activity during magnetic resonance imaging examinations," *J. Biomed. Opt.*, vol. 18, no. 5, May 2013, Art. no. 057006.

[189] Y. Zhao, K. Chen, and J. Yang, "Novel target type flowmeter based on a differential fiber Bragg grating sensor," *Measurement*, vol. 38, no. 3, pp. 230–235, Oct. 2005.

[190] S. Ambastha, S. Umesh, U. Maheshwari K, and S. Asokan, "Pulmonary function test using fiber Bragg grating spirometer," *J. Lightw. Technol.*, vol. 34, no. 24, pp. 5682–5688, Dec. 15, 2016.

[191] J. Yang, X. Chen, and X. Dong, "Hot-wire anemometer based on frosted fiber Bragg grating coated with silver film," in *Proc. IOP Conf. Series Mater. Sci. Eng.*, vol. 711, no. 1, 2020, p. 12112.

[192] R. Gao and D. Lu, "Temperature compensated fiber optic anemometer based on graphene-coated elliptical core micro-fiber Bragg grating," *Opt. Express*, vol. 27, no. 23, p. 34011, Nov. 2019.

[193] Y. Liang, A. P. Mazzolini, and P. R. Stoddart, "Fibre Bragg grating sensor for respiratory monitoring," in *Proc. Austral. Conf. Opt. Fibre Technol./Austral. Opt. Soc. (ACOFT/AOS)*, 2006, pp. 1–6.

[194] A. Manujło and T. Osuch, "Temperature fiber Bragg grating based sensor for respiration monitoring," *Proc. SPIE*, vol. 10445, Aug. 2017, Art. no. 104451A.

[195] D. Lo Presti, C. Massaroni, and E. Schena, "Optical fiber gratings for humidity measurements: A review," *IEEE Sensors J.*, vol. 18, no. 22, pp. 9065–9074, Nov. 2018.

[196] D. Lo Presti, C. Massaroni, V. Piemonte, P. Saccomandi, R. D'Amato, M. A. Caponero, and E. Schena, "Agar-coated fiber Bragg grating sensor for relative humidity measurements: Influence of coating thickness and polymer concentration," *IEEE Sensors J.*, vol. 19, no. 9, pp. 3335–3342, May 2019.

[197] B. Jiang, Z. Bi, Z. Hao, Q. Yuan, D. Feng, K. Zhou, L. Zhang, X. Gan, and J. Zhao, "Graphene oxide-deposited tilted fiber grating for ultrafast humidity sensing and human breath monitoring," *Sens. Actuators B, Chem.*, vol. 293, pp. 336–341, Aug. 2019.

[198] Y. Miao, B. Liu, H. Zhang, Y. Li, H. Zhou, H. Sun, W. Zhang, and Q. Zhao, "Relative humidity sensor based on tilted fiber Bragg grating with polyvinyl alcohol coating," *IEEE Photon. Technol. Lett.*, vol. 21, no. 7, pp. 441–443, Apr. 2009.

[199] C. Massaroni, D. Lo Presti, P. Saccomandi, M. A. Caponero, R. D'Amato, and E. Schena, "Fiber Bragg grating probe for relative humidity and respiratory frequency estimation: Assessment during mechanical ventilation," *IEEE Sensors J.*, vol. 18, no. 5, pp. 2125–2130, Mar. 2018.

[200] C. Massaroni, D. L. Presti, C. Losquadro, P. Resta, P. Saccomandi, E. Schena, R. DrAmato, and M. A. Caponero, "Multi-sensitive FBG-based needle for both relative humidity and breathing rate monitoring," in *Proc. IEEE Int. Symp. Med. Meas. Appl. (MeMeA)*, Jun. 2018, pp. 1–6.

[201] S. P. Morgan, S. Korposh, L. Liu, F. U. Hernandez, R. Correia, A. Norris, R. Sinha, B. R. Hayes-Gill, S. A. Piletsky, F. Canfarotta, E. V. Piletska, and F. Grillo, "Optical fiber sensors for monitoring in critical care," in *Proc. 41st Annu. Int. Conf. IEEE Eng. Med. Biol. Soc. (EMBC)*, Jul. 2019, pp. 1139–1143.

[202] D. L. Presti, C. Massaroni, M. Zaltieri, R. Sabbadini, A. Carnevale, J. Di Tocco, U. G. Longo, M. A. Caponero, R. DAmato, E. Schena, and D. Formica, "A magnetic resonance-compatible wearable device based on functionalized fiber optic sensor for respiratory monitoring," *IEEE Sensors J.*, early access, Mar. 16, 2020, doi: 10.1109/JSEN.2020.2980940.

[203] G. Shafiq and K. C. Veluvolu, "Surface chest motion decomposition for cardiovascular monitoring," *Sci. Rep.*, vol. 4, no. 1, pp. 1–9, May 2014.

[204] K. Chethana, A. S. G. Prasad, S. N. Omkar, and S. Asokan, "Fiber Bragg grating sensor based device for simultaneous measurement of respiratory and cardiac activities," *J. Biophoton.*, vol. 10, no. 2, pp. 278–285, Feb. 2017.

[205] Ł. Dziuda and F. W. Skibniewski, "A new approach to ballistocardiographic measurements using fibre Bragg grating-based sensors," *Biocybern. Biomed. Eng.*, vol. 34, no. 2, pp. 101–116, 2014.

[206] J. Nedoma, M. Fajkus, R. Martinek, and H. Nazeran, "Vital sign monitoring and cardiac triggering at 1.5 tesla: A practical solution by an MR-ballistocardiography fiber-optic sensor," *Sensors*, vol. 19, no. 3, p. 470, Jan. 2019.

[207] S. Koyama, H. Ishizawa, K. Fujimoto, S. Chino, and Y. Kobayashi, "Influence of individual differences on the calculation method for FBG-type blood pressure sensors," *Sensors*, vol. 17, no. 12, p. 48, Dec. 2016.

[208] A. P. Avolio, M. Butlin, and A. Walsh, "Arterial blood pressure measurement and pulse wave analysis—Their role in enhancing cardiovascular assessment," *Physiological Meas.*, vol. 31, no. 1, pp. R1–R47, Jan. 2010.

[209] C. J. Leitão, M. F. Domingues, S. Novais, C. Tavares, J. Pinto, C. Marques, and P. Antunes, "Arterial pulses assessed with FBG based films: A smart skin approach," *Proc. SPIE*, vol. 10685, p. 31, May 2018.

[210] S. Pant, S. Umesh, and S. Asokan, "A novel approach to acquire the arterial pulse by finger plethysmography using fiber Bragg grating sensor," *IEEE Sensors J.*, vol. 20, no. 11, pp. 5921–5928, Jun. 2020.

[211] C. Leitão, L. Bilro, N. Alberto, P. Antunes, H. Lima, P. S. André, R. Nogueira, and J. L. Pinto, "Feasibility studies of Bragg probe for non-invasive carotid pulse waveform assessment," *J. Biomed. Opt.*, vol. 18, no. 1, Jan. 2013, Art. no. 017006.

[212] S. Padma, S. Umesh, T. Srinivas, and S. Asokan, "Carotid arterial pulse waveform measurements using fiber Bragg grating pulse probe," *IEEE J. Biomed. Health Informat.*, vol. 22, no. 5, pp. 1415–1420, Sep. 2018.

[213] D. Jia, J. Chao, S. Li, H. Zhang, Y. Yan, T. Liu, and Y. Sun, "A fiber Bragg grating sensor for radial artery pulse waveform measurement," *IEEE Trans. Biomed. Eng.*, vol. 65, no. 4, pp. 839–846, Apr. 2018.

[214] S. Chino, H. Ishizawa, S. Hosoya, S. Koyama, K. Fujimoto, and T. Kawamura, "Research for wearable multiple vital sign sensor using fiber Bragg grating—Verification of several pulsate points in human body surface," in *Proc. IEEE Int. Instrum. Meas. Technol. Conf. (I2MTC)*, May 2017, pp. 1–6.

[215] Y. Haseda, J. Bonefacino, H.-Y. Tam, S. Chino, S. Koyama, and H. Ishizawa, "Measurement of pulse wave signals and blood pressure by a plastic optical fiber FBG sensor," *Sensors*, vol. 19, no. 23, p. 5088, Nov. 2019.

[216] Y. Miyauchi, S. Koyama, and H. Ishizawa, "Basic experiment of blood-pressure measurement which uses FBG sensors," in *Proc. IEEE Int. Instrum. Meas. Technol. Conf. (I2MTC)*, May 2013, pp. 1767–1770.

[217] Y. Katsuragawa and H. Ishizawa, "Non-invasive blood pressure measurement by pulse wave analysis using FBG sensor," in *Proc. IEEE Int. Instrum. Meas. Technol. Conf. (I2MTC)*, May 2015, pp. 511–515.

[218] S. Koyama, H. Ishizawa, A. Sakaguchi, S. Hosoya, and T. Kawamura, "Influence on calculated blood pressure of measurement posture for the development of wearable vital sign sensors," *J. Sensors*, vol. 2017, pp. 1–10, 2017.

[219] A. van Brakel, P. L. Swart, A. A. Chtcherbakov, and M. G. Shlyagin, "Blood pressure manometer using a twin Bragg grating Fabry–Perot interferometer," *Proc. SPIE*, vol. 5634, p. 595, Feb. 2005.

[220] U. Sharath, R. Sukreet, G. Apoorva, and S. Asokan, "Blood pressure evaluation using sphygmomanometry assisted by arterial pulse waveform detection by fiber Bragg grating pulse device," *J. Biomed. Opt.*, vol. 18, no. 6, Jun. 2013, Art. no. 067010.

[221] H. Li, H. Yang, E. Li, Z. Liu, and K. Wei, "Wearable sensors in intelligent clothing for measuring human body temperature based on optical fiber Bragg grating," *Opt. Express*, vol. 20, no. 11, p. 11740, May 2012.

[222] Q. Yu, Y. Zhang, Y. Dong, Y. P. Li, C. Wang, and H. Chen, "Study on optical fiber Bragg grating temperature sensors for human body temperature monitoring," in *Proc. Symp. Photon. Optoelectron. (SOPO)*, May 2012, pp. 1–4.

[223] L. D'Acquisto, F. Scardulla, and S. Pasta, "Steam sterilization processes affect the stability of clinical thermometers: Thermistor and prototypal FBG probe comparison," *Opt. Fiber Technol.*, vol. 55, Mar. 2020, Art. no. 102156.

[224] W. Xu, D. Wang, D. Li, and C. C. Liu, "Recent developments of electrochemical and optical biosensors for antibody detection," *Int. J. Mol. Sci.*, vol. 21, no. 1, p. 134, Dec. 2019.

[225] C. Chen and J. Wang, "Optical biosensors: An exhaustive and comprehensive review," *Analyst*, vol. 145, no. 5, pp. 1605–1628, Mar. 2020.

[226] X. D. Wang and O. S. Wolfbeis, "Fiber-optic chemical sensors and biosensors (2015–2019)," *Anal. Chem.*, vol. 92, no. 1, pp. 397–430, Jan. 2020.

[227] B. N. Shivananju, M. Renilkumar, G. R. Prashanth, S. Asokan, and M. M. Varma, "Detection limit of etched fiber Bragg grating sensors," *J. Lightw. Technol.*, vol. 31, no. 14, pp. 2441–2447, Jul. 2013.

[228] M. Loyez, E. M. Hassan, M. Lobry, F. Liu, C. Caucheteur, R. Wattiez, M. C. DeRosa, W. G. Willmore, and J. Albert, "Rapid detection of circulating breast cancer cells using a multiresonant optical fiber aptasensor with plasmonic amplification," *ACS Sensors*, vol. 5, no. 2, pp. 454–463, Feb. 2020.

[229] J. Lao, L. Han, Z. Wu, X. Zhang, Y. Huang, Y. Tang, and T. Guo, "Gold nanoparticle-functionalized surface plasmon resonance optical fiber biosensor: *In situ* detection of thrombin with 1 n·M detection limit," *J. Lightw. Technol.*, vol. 37, no. 11, pp. 2748–2755, Jun. 1, 2019.

[230] W. Hu, Y. Huang, C. Chen, Y. Liu, T. Guo, and B.-O. Guan, "Highly sensitive detection of dopamine using a graphene functionalized plasmonic fiber-optic sensor with aptamer conformational amplification," *Sens. Actuators B, Chem.*, vol. 264, pp. 440–447, Jul. 2018.

[231] A. Candiani, M. Sozzi, A. Cucinotta, S. Selleri, R. Veneziano, R. Corradini, R. Marchelli, P. Childs, and S. Pissadakis, "Optical fiber ring cavity sensor for label-free DNA detection," *IEEE J. Sel. Topics Quantum Electron.*, vol. 18, no. 3, pp. 1176–1183, May 2012.

[232] A. N. Chryssis, S. S. Saini, S. M. Lee, H. Yi, W. E. Bentley, and M. Dagenais, "Detecting hybridization of DNA by highly sensitive evanescent field etched core fiber Bragg grating sensors," *IEEE J. Sel. Topics Quantum Electron.*, vol. 11, no. 4, pp. 864–872, Jul. 2005.

[233] A. Revzin, E. Maverakis, and H.-C. Chang, "Biosensors for immune cell analysis—A perspective," *Biomicrofluidics*, vol. 6, no. 2, Jun. 2012, Art. no. 021301.

[234] V. Malachovská, C. Ribaut, V. Voisin, M. Surin, P. Leclère, R. Wattiez, and C. Caucheteur, "Fiber-optic SPR immunosensors tailored to target epithelial cells through membrane receptors," *Anal. Chem.*, vol. 87, no. 12, pp. 5957–5965, Jun. 2015.

[235] C. Caucheteur, V. Malachovska, C. Ribaut, and R. Wattiez, "[INVITED] cell sensing with near-infrared plasmonic optical fiber sensors," *Opt. Laser Technol.*, vol. 78, pp. 116–121, Apr. 2016.

[236] H. M. H. Hurks, J. A. W. Metzelaar-Blok, E. R. Barthen, A. H. Zwinderman, D. D. Wolff-Rouendaal, J. E. E. Keunen, and M. J. Jager, "Expression of epidermal growth factor receptor: Risk factor in uveal melanoma," *Invest. Ophthalmol. Vis. Sci.*, vol. 41, no. 8, pp. 2023–2027, 2000.

[237] Y. Shevchenko, T. J. Francis, D. A. D. Blair, R. Walsh, M. C. DeRosa, and J. Albert, "*In situ* biosensing with a surface plasmon resonance fiber grating aptasensor," *Anal. Chem.*, vol. 83, no. 18, pp. 7027–7034, Sep. 2011.

[238] X. Chen, Y. Nan, X. Ma, H. Liu, W. Liu, L. Shi, and T. Guo, "*In-situ* detection of small biomolecule interactions using a plasmonic tilted fiber grating sensor," *J. Lightw. Technol.*, vol. 37, no. 11, pp. 2792–2799, Jun. 1, 2019.

[239] B. Jiang, K. Zhou, C. Wang, Q. Sun, G. Yin, Z. Tai, K. Wilson, J. Zhao, and L. Zhang, "Label-free glucose biosensor based on enzymatic graphene oxide-functionalized tilted fiber grating," *Sens. Actuators B, Chem.*, vol. 254, pp. 1033–1039, Jan. 2018.

[240] B. Luo, Z. Yan, Z. Sun, Y. Liu, M. Zhao, and L. Zhang, "Biosensor based on excessively tilted fiber grating in thin-cladding optical fiber for sensitive and selective detection of low glucose concentration," *Opt. Express*, vol. 23, no. 25, p. 32429, Dec. 2015.

[241] C. Massaroni, P. Saccomandi, D. Formica, D. Lo Presti, M. A. Caponero, G. Di Tomaso, F. Giurazza, M. Muto, and E. Schena, "Design and feasibility assessment of a magnetic resonance-compatible smart textile based on fiber Bragg grating sensors for respiratory monitoring," *IEEE Sensors J.*, vol. 16, no. 22, pp. 8103–8110, Nov. 2016.

[242] D. Q. Larkin and D. C. Shafer, "Robotic surgery system including position sensors using fiber Bragg gratings," U.S. Patent 7 930 065 B2, Apr. 19, 2011.

[243] Y. L. Park, R. J. Black, B. Moslehi, M. R. Cutkosky, S. Elayaperumal, B. Daniel, A. Yeung, V. Sotoudeh, "Steerable shape sensing biopsy needle and catheter," U.S. Patent 8 649 847 B1, Feb. 11, 2014.

[244] D. E. Kerr and W. H. Nau, Jr., "Surgical instrument with fiber Bragg grating," U.S. Patent 9 113 904 B2, Aug. 25, 2015.

[245] F. H. Moll and R. L. Schlesinger, "Robotic surgical instrument and methods using Bragg fiber sensors," U.S. Patent 0 218 770 A1, Sep. 11, 2008.

DANIELA LO PRESTI (Student Member, IEEE) received the M.Sc. degree in 2016. She is currently pursuing the Ph.D. degree in bioengineering with the Università Campus Bio-Medico di Roma (UCBM). Her research interests include the design, fabrication, and assessment of FBGs-based systems for medical and biomedical applications.

CARLO MASSARONI (Member, IEEE) received the Ph.D. degree in 2017. He is currently an Assistant Professor of measurements with UCBM. His research interests include the design, development, and test of wearable devices and unobtrusive measuring systems for medical applications. He has been an Associate Member of the TC on Wearable Biomedical Sensors and Systems of the IEEE EMBS since 2019. He has also been the Chair of the Wearable Sensors TC of the Italy Chapter of the IEEE Sensors Council since 2020.

CÁTIA SOFIA JORGE LEITÃO received the Ph.D. degree in 2017. She is currently the Postdoctoral Researcher with the Nanophotonics and Optoeletronics Group of i3N, Department of Physics, University of Aveiro, in collaboration with the Instituto de Telecomunicações. Her current research interests include the study and development of photonic and optoelectronic solutions for biomedical sensing, especially based on optical fiber sensors.

MARIA DE FÁTIMA DOMINGUES (Member, IEEE) received the Ph.D. degree in 2015. She is currently a Researcher with the Instituto de Telecomunicações, University of Aveiro. She is authored and coauthored more than 80 journal and conference papers, chapters, and books. At present, her current research interests embrace new solutions of optical fiber based sensors and its application in e-Health scenarios, with a focus in physical rehabilitation architectures.

MARZHAN SYPABEKOVA received the Ph.D. degree in 2019. She is currently working as a Postdoctoral Associate with the School of Medicine, Nazarbayev University, Nur-Sultan, Kazakhstan. She has experience in developing biosensors (electrochemical and fiber optic), molecular and cellular biology, and bioengineering.

DAVID BARRERA received the Ph.D. degree in 2013. He is currently a Postdoctoral Researcher with the Department of Electronics, University of Alcalá. His current research interests include optical fiber sensors, fiber Bragg grating sensors, and multicore optical fibers.

IGNAZIO FLORIS received the Ph.D. degree in 2020. He is currently working as an Early Stage Researcher (ESR) with the European Innovative Training Network FINESSE (FIbre NErvous Sensing SystEms), Institute of Concrete Science and Technology (ICITECH), and with the Institute of Telecommunications and Multimedia Applications (iTEAM), Universitat Politècnica de València. His research interests include civil engineering, fiber optic sensors, and data analysis.

LUCA MASSARI received the Ph.D. degree in 2019. He is currently with the Neuro-Robotic Touch Laboratory, Scuola Superiore Sant'Anna (SSSA), serving as a Postdoctoral Researcher. He has been working in several National projects (TUNE-BEAM, SENSE-RISC, Centauro, IMEROS, Parloma Smart Cities, and Social Innovation call) and EU-H2020 projects (Neuheart and Endoo) serving as the Project Manager in some of them. His research interests include development of large area sensing skin and haptic interfaces for biorobotic fields, such as medical robotics, wearable technologies, and collaborative robotics.

CALOGERO MARIA ODDO (Senior Member, IEEE) received the Ph.D. degree in 2011. He is currently an Associate Professor of bioengineering with SSSA, Pisa, Italy. He coordinates the Neuro-Robotic Touch Laboratory (about 20 research fellows), The BioRobotics Institute, SSSA, with a growing track record in integrating biorobotics and neuroscience, with particular interests in the study of the human sense of touch and on its artificial engineering.

SALVADOR SALES (Senior Member, IEEE) received the Ph.D. degree in 1995. He has been a Professor with the ITEAM Research Institute, Universitat Politècnica de València, Spain, since 2007. He was recognized with the Annual Award of the Spanish Telecommunication Engineering Association to the best Ph.D. on optical communications. He has been involved some national and European research, and coauthor of more than 250 journal articles. His main research interests include optoelectronic signal processing, optical delay lines, fiber Bragg gratings, WDM and SCM lightwave systems, and semiconductor optical amplifiers.

IULIAN IOAN IORDACHITA (Senior Member, IEEE) received the Ph.D. degree in 1996. He is currently a Faculty Member of the Laboratory for Computational Sensing and Robotics, Johns Hopkins University, and the Director of the Advanced Medical Instrumentation and Robotics Research Laboratory. His current research interests include medical robotics, image guided surgery, robotics, smart surgical tools, and medical instrumentation.

DANIELE TOSI received the Ph.D. degree in 2010. He is currently an Associate Professor of electrical and computer engineering with Nazarbayev University, and the Head of the Biosensors and Bioinstruments Laboratory, National Laboratory Astana. His research interests include optical fiber sensors, biomedical sensors, distributed sensing, and biosensors. He was a recipient of the IEEE Sensors Council Early Career Technical Award in 2018. He is also an Associate Editor of the IEEE Sensors Journal.

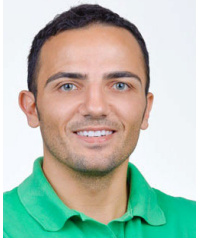

EMILIANO SCHENA (Senior Member, IEEE) received the Ph.D. degree in 2007. He is currently an Associate Professor of measurements with the Università Campus Bio-Medico di Roma. His research interests include the design and assessment of wearable systems for vital signs monitoring. He became the Chair of the Italy Chapter of the IEEE Sensors Council in 2018.